29. Egami T, Sando I, Black FO. Hypoplasia of the vestibular aqueduct and endolymphatic sac in endolymphatic hydrops. ORL 1978;86:327–339.
30. Kusakari J, Kobayashi T, Arakawa E, *et al.* Time-realted changes in cochlear potentials in guinea pigs with experimentally induced endolymphatic hydrops. Acta Oto-Laryngol Suppl 1987;435:27–33.
31. Kitahara M, Takeda T, Yazawa Y, *et al.* Experimental study on Meniere's disease. Otolaryngol Head Neck Surg 1982;90:470–481.
32. Nishimura M, Kakigi A, Takeda T, *et al.* Time course changes of vasopressin-induced enlargement of the rat intrastrial space and the effects of a vasopressin type 2 antagonist. Acta Oto-Laryngol 2009; 129:709–715.
33. Merchant SN, Adams JC, Nadol Jr JB. Pathophysiology of Meniere's syndrome: are symptoms caused by endolymphatic hydrops? Otol Neurotol, 2005;26:74–81.
34. Lin MY, Timmer FC, Oriel BS, *et al.* Vestibular evoked myogenic potentials (VEMP) can detect asymptomatic saccular hydrops. Laryngoscope 2006;116:987–992.
35. Morita N, Cureoglu S, Nomiya S, *et al.* Potential cause of positional vertigo in Ménière's disease. Otol Neurotol 2009;30:956–960.
36. Kato M, Teranishi M, Katayama N, *et al.* Association between endolymphatic hydrops as revealed by magnetic resonance imaging and caloric response. Otol Neurotol 2011;32:1480–1485.
37. Steel KP. Perspectives: biomedicine. The benefits of recycling. Science 1999;285:1363–1364.
38. Sterkers O, Ferrary E, Amiel C. Production of inner ear fluids. Physiol Rev 1988;68:1083–1128.
39. Sawada S, Takeda T, Kitano H, *et al.* Auaporin-2 regulation by vasopressin in the rat inner ear. NeuroReport 2002;13:1127–1129.
40. Hornibrool J, George P, Gourley J. Vasopressin in definite Meniere's disease with positive electrocochleographic findings. Acta Otolaryngol 2011;131:613–617.
41. Robertson GL, Mahr EA, Athar S, *et al.* The development and clinical application of a new radioimmunoassay for arginine–vasopressin in human plasma. J Clin Invest 1973;52:2340–2352.
42. Nussey SS, Ang VT, Bevan DH, *et al.* Human platelet arginine vasopressin. Clin Endocrinol 1986;24:427–433.
43. Bichet DG, Arthus MF, Barjon JN, *et al.* Human platelet fraction arginine-vasopressin. Potential physiological role. J Clin Invest 1987; 79:881–887.
44. Furuta H, Luo L, Ryan AF, *et al.* Expression of mRNA encoding vasopressin V1a, vasopressin V2, and ANP-B receptors in the rat cochlea. Hear Res 1998;117:140–148.
45. Furuta H, Sato C, Kawaguchi Y, *et al.* Expression of mRNAs encoding hormone receptors in the endolymphatic sac of the rat. Acta Otolaryngol 1999;119:53–57.
46. Fukushima K, Takeda T, Kakigi A, *et al.* Effects of lithium on endolymph homeostasis and experimentally induced endolymphatic hydrops. ORL 2005;67:282–288.

Expression analysis of microRNAs in murine cochlear explants

Misato Hirai, Yukihide Maeda, Kunihiro Fukushima, Akiko Sugaya, Yuko Kataoka and Kazunori Nishizaki

MicroRNAs (miRNAs) play functional roles in sound transduction in cochlea. This study focuses on the validity of cochlear culture as an *in vitro* experimental tool, in view of miRNA expression. E15 cochleae were dissected and maintained *in vitro* for 48 h before extraction of miRNAs. MiRNA expression was comprehensively screened in explanted cochleae using a miRNA array that covers 380 miRNAs. A strong correlation was observed between expression levels of miRNAs in *in vitro* and in *in vivo* cochleae. Levels of 43 miRNAs were altered *in vitro* and these changes were reproducible over three trials. These findings indicate that *in vitro* miRNA profiling is a viable method for analysis of gene expression and action of chemical compounds on cochleae.

NeuroReport 22:652–654 © 2011 Wolters Kluwer Health | Lippincott Williams & Wilkins.

NeuroReport 2011, 22:652–654

Keywords: embryonic cochlea, microRNA array, organ culture of cochlea

Department of Otolaryngology-, Head and Neck Surgery, Okayama University Graduate School of Medicine, Dentistry and Pharmacy, Okayama, Japan

Correspondence to Yukihide Maeda, MD, PhD, Department of Otolaryngology, Head and Neck Surgery, Okayama University Graduate School of Medicine, Dentistry and Pharmacy, 2-5-1 Shikata-cho, Kita-wand, Okayama, Japan, 700-8558
Tel: +81 086 235 7307; fax: +81 86 235 7308;
e-mail: maedayj@yahoo.co.jp

Received 6 June 2011 accepted 16 June 2011

Introduction

Cochlear culture is a useful tool to investigate the expression of genes [1] and the actions of chemical compounds on the cochlea. For example, it has been used for investigations of cochlea-specific gene expressions [1] and those for action of dexamethasone on cochlear tissue [2]. Recent studies have found that the expression of particular microRNAs (miRNAs) plays critical roles in cochlear function [3–8]. We have already reported that miRNA expression in cochlear explants is well-preserved under the *in vitro* experimental conditions, as shown by DNA microarray assay [2]. However, the mechanism by which the expression of miRNAs is maintained *in vivo* is unknown. As a first step, it is important to test the validity of cochlear culture in view of miRNA expression as an *in vitro* experimental tool. In this study, the expression of miRNAs in cochlear explants was comprehensively evaluated using a miRNA array that covers 380 miRNAs, and the miRNAs were compared between *in vitro* and *in vivo* conditions.

Materials and methods

Tissue dissection and culture of mouse cochleae

Timed pregnant female BALB/c mice were killed using an excess of ketamine (150 mg/kg, intraperitoneally) on E15 (vaginal plug, E0). The fetal cochleae were immediately dissected under a binocular microscope and frozen in liquid nitrogen until total RNA extraction, or placed into Dulbecco's modified Eagle's medium supplemented with 5% KnockOut Serum Replacement (Invitrogen, Carlsbad, California, USA) and penicillin G (0.06 mg/ml). The explanted cochlea included the cochlear duct and immature sensory epithelium, nonneuronal mesenchymal tissues, lateral wall of the cochlea, and spiral neurons [2].

Explanted cochleae were placed in 250 μl of serum-free medium and maintained at 37°C in 5% CO_2, with daily serum changes. Explanted cochleae were maintained *in vitro* for 48 h (DIV2: Day *In Vitro* 2) before extraction of total RNA. In general, 12–14 cochleae from a single litter were processed in each sample. All experimental protocols complied with the guidelines of the Okayama University's Committee on the Use and Care of Animals.

Comprehensive analysis of microRNA expression in cochlear tissue

To screen miRNA expression in the explanted cochleae, we carried out a microarray analysis using *mir*Vana miRNA Bioarray V9.2 (Filgen, Inc., Aichi, Japan). This microarray carries the nucleotides for a total of 380 miRNAs with each miRNA spotted in quadruplicate. MiRNA purification and other experimental procedures were performed as follows:

MiRNA purification and labeling

Total RNA was extracted from the *in vitro* and *in vivo* cochlear tissues using an RNA-easy column (Qiagen, Hilden, Germany). The quality of the purified RNA was checked using an Agilent 2100 Bioanalyzer (Agilent Technologies, Tokyo, Japan). Using the flash PAGE system (Ambion Inc., Austin, Texas, USA), we purified the miRNAs from 22 μg of total RNA. The purified miRNA was labeled using a *mir*Vana miRNA Labeling Kit (Ambion Inc.) and CyDye Mono-Reactive Dye Pack (GE Healthcare Bio-science Corp., Piscataway, New Jersey, USA) according to the manufacturer's protocol.

0959-4965 © 2011 Wolters Kluwer Health | Lippincott Williams & Wilkins DOI: 10.1097/WNR.0b013e32834a0273

Hybridization to miRNA array and data analysis

The labeled miRNAs were dissolved in 1× miRNA hybridization buffer, incubated for 3 min at 95°C and then cooled to room temperature before application to the arrays. The arrays were then incubated for 16–20 h at 42°C. After hybridization, the arrays were washed once with low stringency wash (nuclease-free water = 376 ml, detergent concentrate = 4 ml, salt concentrate = 20 ml) for 30 s and twice with high stringency wash (nuclease-free water = 780 ml, salt concentrate = 20 ml) for 30 s. After the arrays were centrifuged at 600*g* for 5 min for drying, they were scanned using a GenePix 4000B scanner (Axon Instruments, Sunnyvale, California, USA) and the signal data of each array was calculated using an Array-Pro Analyzer version 4.5 (Media Cybernetics Inc., Bethesda, Maryland, USA). The array data was normalized and averaged using the Microarray Data Analysis Tool (Filgen, Nagoya, Japan). All the experiments, including tissue dissection, cochlear culture, and miRNA extraction and hybridization on the array, were performed three times to test the reproducibility of the results.

Results

The overall correlation of the expression of the 380 miRNAs between the *in vitro* and *in vivo* cochleae was very high ($r = 0.902$, $P < 0.001$) (Fig. 1). However, several miRNAs were expressed differently in the cochlear culture. Among these, 27 miRNAs had increased by more than two-fold and 37 miRNAs had decreased to less than half in the *in vitro* cochlear tissue compared with the *in vivo* cochleae in the first trial of the experiment. In the second trial, the expression levels of 30 miRNAs had increased and that of 43 miRNAs had decreased, while in the third trial, 29 miRNAs had increased and 40 miRNAs had decreased. In each of the three trials, the expression level of 19 particular miRNAs always increased by more than two-fold and that of 23 particular miRNAs always decreased to less than half, with striking reproducibility (Table 1).

Fig. 1

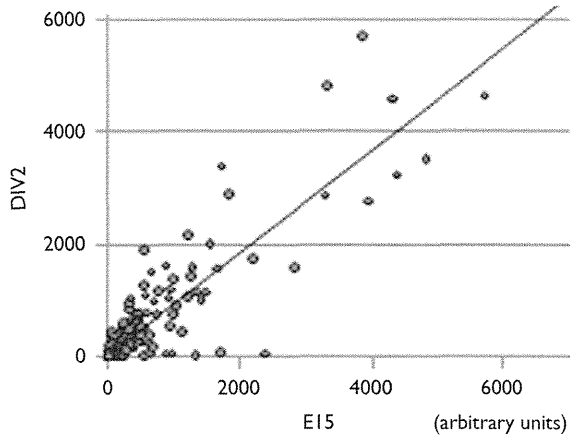

Overall levels of microRNA expressions in the cochleae before and after explantation. The overall expression levels of the 380 miRNAs were highly correlated between the *in vitro* and *in vivo* cochleae ($r = 0.902$, $P < 0.001$).

Discussion

This data demonstrates that the overall expression levels of miRNAs before and after explantation are strongly correlated. A small number of miRNAs demonstrated differential expression after explantation but these changes in the expression levels occurred with striking reproducibility throughout the three trials. Our data validates the use of cochlear explants as a model to investigate gene expressions and the actions of various chemical compounds on cochlear tissue.

In this study, the expression level of 19 miRNAs increased while that of 23 miRNAs decreased *in vitro* in all three trials with 100% reproducibility.

Among them, the expression level of miR-762 (gene ID: 791073) always decreased. This miRNA is known to interact and inactivate the expression of Hsf1 (gene ID: 15499, heat-shock factor 1, MicroCosm Targets, *http://www.ebi.ac.uk/enright-srv/microcosm*). This protein activates heat-shock response genes under conditions of heat or other stresses such as hypoxia [9]. We previously examined miRNA expression in cochlear explants and reported that the expression level of *Gapdh* is increased in explanted cochleae, indicating that cochlear tissue in culture is in a state of relative hypoxia [1]. We believe that the expression level of miR-762 may have changed in response to the hypoxic conditions.

The expression levels of miR-22 (gene ID: 387141) and miR-683 (gene ID: 751559) decreased in all three trials of the experiment. MiR-22 is known to interact and inactivate the expression of Dad1 (gene ID: 13135, defender against cell death 1, MicroCosm Targets). MiR-683 is known to interact and inactivate the expression of Aven (gene ID: 74268, apoptosis, caspase activation inhibitor, MicroCosm Targets). These proteins have been shown to play roles in preventing apoptotic cell death [10,11], suggesting that the reduction in the expression levels of miR-22 and miR-683 may lead to prevention of apoptotic cell death. These miRNAs are thought to be regulated in cochlear explants as a protective response to the exposure of the tissue to *in vitro* conditions.

Conclusion

MiRNAs are important regulators of many cellular functions due to their ability to bind to and inhibit specific miRNAs [4,12]. Therefore, the validity of the cochlear explant as an *in vitro* experimental tool with regard to miRNA expression must be established.

We found a strong correlation in the expression levels of miRNAs between *in vitro* and *in vivo* cochleae ($r = 0.902$, $P < 0.001$). The levels of 43 of the 380 miRNAs screened were altered *in vitro* but these changes were

Table 1 MicroRNAs increased by more than two-fold or decreased to less than half in the *in vitro* cochleae compared with the *in vivo* cochleae

	Ratio of normalized intensity				Ratio of normalized intensity		
MicroRNAs increased by more than two-fold *in vitro*	First trial	Second trial	Third trial	MicroRNAs decreased by less than 0.5-fold *in vitro*	First trial	Second trial	Third trial
miR-20a	2.03	2.46	2.33	miR-224	0.24	0.43	0.38
miR-106b	2.29	2.93	2.56	miR-297	0.09	0.07	0.04
miR-92	2.76	2.64	2.83	miR-341	0.23	0.23	0.24
miR-181a	2.16	2.06	2.20	miR-34a	0.33	0.38	0.40
miR-106a	2.13	2.54	2.35	miR-22	0.36	0.34	0.40
miR-18	3.62	5.12	5.12	miR-346	0.17	0.12	0.14
miR-19b	2.49	2.75	2.91	miR-468	0.04	0.03	0.02
miR-19a	2.50	2.01	2.88	miR-370	0.49	0.48	0.41
miR-124a	5.82	7.71	6.76	miR-210	0.30	0.35	0.32
miR-126-3p	3.82	5.31	3.52	miR-204	0.19	0.15	0.40
miR-301	2.52	2.00	4.04	miR-122a	0.16	0.12	0.10
miR-20b	2.09	2.63	2.45	miR-26b	0.34	0.23	0.47
miR-503	2.72	2.91	3.21	let-7f	0.29	0.26	0.40
miR-302c	2.44	2.25	3.76	miR-669b	0.05	0.04	0.03
miR-720	2.22	2.20	2.51	miR-679	0.35	0.47	0.35
miR-690	2.63	3.01	2.31	miR-297b	0.11	0.07	0.05
miR-138	4.59	4.74	3.57	miR-683	0.27	0.23	0.35
miR-301b	2.38	2.79	4.13	miR-669c	0.03	0.02	0.02
miR-804	3.10	3.61	4.00	miR-669a	0.08	0.06	0.05
				miR-711	0.43	0.28	0.37
				miR-672	0.14	0.10	0.07
				miR-762	0.37	0.35	0.24
				miR-760	0.46	0.47	0.35

The expression of 19 miRNAs was upregulated by more than two-fold, and that of 23 miRNAs was downregulated to less than half *in vitro*, compared with the levels *in vivo*. These data were completely reproducible over the three experimental trials.

highly reproducible over the three experimental trials. Changes in the levels of several miRNAs, such as miR-762, miR-22, and miR-683, are thought to be a protective response to hypoxia and apoptosis *in vitro*. These findings indicate the validity of using cochlear explants for investigations with regard to gene expression and the actions of various chemical compounds on the cochlea.

Acknowledgements

This work was supported by a grant from the Japanese Ministry of Health, Labour and Welfare (H23-NANCHI-IPPAN-021).

Conflict of interest

There is no conflict of interest for this manuscript, including financial, consultant, and other relations.

References

1 Maeda Y, Fukushima K, Kakiuchi M, Orita Y, Nishizaki K, Smith RJ. RT-PCR analysis of Tecta, Coch, Eya4 and Strc in mouse cochlear explants. *Neuroreport* 2005; **16**:361–365.
2 Maeda Y, Fukushima K, Hirai M, Kariya S, Smith RJ, Nishizaki K. Microarray analysis of the effect of dexamethasone on murine cochlear explants. *Acta Otolaryngol* 2010; **130**:1329–1334.
3 Li H, Kloosterman W, Fekete DM. MicroRNA-183 family members regulate sensorineural fates in the inner ear. *J Neurosci* 2010; **30**:3254–3263.
4 Tsonis PA, Call MK, Grogg MW, Sartor MA, Taylor RR, Forge A, *et al.* MicroRNAs and regeneration: Let-7 members as potential regulators of dedifferentiation in lens and inner ear hair cell regeneration of the adult newt. *Biochem Biophys Res Commun* 2007; **362**:940–945.
5 Weston MD, Pierce ML, Rocha-Sanchez S, Beisel KW, Soukup GA. MicroRNA gene expression in the mouse inner ear. *Brain Res* 2006; **1111**:95–104.
6 Mencia A, Modamio-Hoybjor S, Redshaw N, Morin M, Mayo-Merino F, Olavarrieta L, *et al.* Mutations in the seed region of human miR-96 are responsible for nonsyndromic progressive hearing loss. *Nat Genet* 2009; **41**:609–613.
7 Soukup GA, Fritzsch B, Pierce ML, Weston MD, Jahan I, McManus MT, *et al.* Residual microRNA expression dictates the extent of inner ear development in conditional Dicer knockout mice. *Dev Biol* 2009; **328**:328–341.
8 Weston MD, Soukup GA. MicroRNAs sound off. *Genome Med* 2009; **1**:59.
9 Kang MJ, Jung SM, Kim MJ, Bae JH, Kim HB, Kim JY, *et al.* DNA-dependent protein kinase is involved in heat shock protein-mediated accumulation of hypoxia-inducible factor-1alpha in hypoxic preconditioned HepG2 cells. *FEBS J* 2008; **275**:5969–5981.
10 Hong NA, Flannery M, Hsieh SN, Cado D, Pedersen R, Winoto A. Mice lacking Dad1, the defender against apoptotic death-1, express abnormal N-linked glycoproteins and undergo increased embryonic apoptosis. *Dev Biol* 2000; **220**:76–84.
11 Kutuk O, Temel SG, Tolunay S, Basaga H. Aven blocks DNA damage-induced apoptosis by stabilising Bcl-xL. *Eur J Cancer* 2010; **46**:2494–2505.
12 Kutty RK, Samuel W, Jaworski C, Duncan T, Nagineni CN, Raghavachari N, *et al.* MicroRNA expression in human retinal pigment epithelial (ARPE-19) cells: increased expression of microRNA-9 by N-(4-hydroxyphenyl)retinamide. *Mol Vis* 2010; **16**:1475–1486.

OPEN ACCESS Freely available online

PLOS | ONE

Time Courses of Changes in Phospho- and Total- MAP Kinases in the Cochlea after Intense Noise Exposure

Yukihide Maeda*, Kunihiro Fukushima, Ryotaro Omichi, Shin Kariya, Kazunori Nishizaki

Department of Otolaryngology – Head and Neck Surgery, Okayama University Graduate School of Medicine, Dentistry and Pharmacy, Okayama, Japan

Abstract

Mitogen-activated protein kinases (MAP kinases) are intracellular signaling kinases activated by phosphorylation in response to a variety of extracellular stimuli. Mammalian MAP kinase pathways are composed of three major pathways: MEK1 (mitogen-activated protein kinase kinase 1)/ERK 1/2 (extracellular signal-regulated kinases 1/2)/p90 RSK (p90 ribosomal S6 kinase), JNK (c-Jun amino (N)-terminal kinase)/c-Jun, and p38 MAPK pathways. These pathways coordinately mediate physiological processes such as cell survival, protein synthesis, cell proliferation, growth, migration, and apoptosis. The involvement of MAP kinase in noise-induced hearing loss (NIHL) has been implicated in the cochlea; however, it is unknown how expression levels of MAP kinase change after the onset of NIHL and whether they are regulated by transient phosphorylation or protein synthesis. CBA/J mice were exposed to 120-dB octave band noise for 2 h. Auditory brainstem response confirmed a component of temporary threshold shift within 0–24 h and significant permanent threshold shift at 14 days after noise exposure. Levels and localizations of phospho- and total- MEK1/ERK1/2/p90 RSK, JNK/c-Jun, and p38 MAPK were comprehensively analyzed by the Bio-Plex® Suspension Array System and immunohistochemistry at 0, 3, 6, 12, 24 and 48 h after noise exposure. The phospho-MEK1/ERK1/2/p90 RSK signaling pathway was activated in the spiral ligament and the sensory and supporting cells of the organ of Corti, with peaks at 3–6 h and independently of regulations of total-MEK1/ERK1/2/p90 RSK. The expression of phospho-JNK and p38 MAPK showed late upregulation in spiral neurons at 48 h, in addition to early upregulations with peaks at 3 h after noise trauma. Phospho-p38 MAPK activation was dependent on upregulation of total-p38 MAPK. At present, comprehensive data on MAP kinase expression provide significant insight into understanding the molecular mechanism of NIHL, and for developing therapeutic models for acute sensorineural hearing loss.

Citation: Maeda Y, Fukushima K, Omichi R, Kariya S, Nishizaki K (2013) Time Courses of Changes in Phospho- and Total- MAP Kinases in the Cochlea after Intense Noise Exposure. PLoS ONE 8(3): e58775. doi:10.1371/journal.pone.0058775

Editor: Bernd Sokolowski, University of South Florida, United States of America

Received December 21, 2012; **Accepted** February 6, 2013; **Published** March 6, 2013

Funding: This work was supported by grants from Japanese Ministry of Health, Labour and Welfare (H23-NANCHI-IPPAN-021; http://www.mhlw.go.jp/) and Japanese Ministry of Education, Culture, Sports, Science and Technology (KAKEN 22591880; http://www.mext.go.jp/). The funders had no role in study design, data collection and analysis, decision to publish, or preparation of the manuscript.

Competing Interests: The authors have declared that no competing interests exist.

* E-mail: maedayj@yahoo.co.jp

Introduction

Noise-induced hearing loss (NIHL) is a major form of acute sensorineural hearing loss (SNHL). The audiological features and cochlear morphology of NIHL are well characterized, but the molecular process in the development of NIHL is not well-elucidated in the cochlea. In an animal study [1], exposure of mice to 120-dB octave band noise for 2 h resulted in immediate elevation of the auditory brainstem response (ABR) threshold and partial recovery of hearing at 24 h after the noise exposure. The ABR threshold showed no significant change after 24 h, 3 days, 1 week, 2 weeks, and 8 weeks. Stabilization of a permanent threshold shift was confirmed at 2 weeks post-noise exposure.

Mitogen-activated protein kinases (MAP kinases) are serine/threonine-specific protein kinases that are activated by phosphorylation in response to a variety of extracellular stimuli. Conventional MAP kinases comprise three intracellular signaling pathways: MEK1 (mitogen-activated protein kinase kinase 1)/ERK 1/2 (extracellular signal-regulated kinases 1/2)/p90 RSK (p90 ribosomal S6 kinase), JNK (c-Jun amino (N)-terminal kinase)/c-Jun, and p38 MAPK pathways. These pathways coordinately regulate gene expression, mitosis, metabolism, motility, cell survival, apoptosis, and differentiation [2]. Sequential phosphorylation of MEK1/ERK1/2/p90 RSK is induced by growth factors, including platelet-derived growth factor, epidermal growth factor and nerve growth factor, cytokines, osmotic stress, and microtubule disorganization [3]. JNK/c-Jun phosphorylation is promoted by stress stimuli including heat shock, ionizing radiation, oxidative stress, DNA-damaging agents, cytokines, UV irradiation, and protein synthesis inhibitors [4]. The p38 MAPK pathway is also strongly activated by various environmental stresses, such as oxidative stress, hypoxia, ischemia, and UV irradiation [5].

The involvement of the MAP kinase pathways in NIHL is suggested by alteration in the cochlear expressions of phosphorylated MAP kinases after intense noise exposure, which causes a temporary or permanent threshold shift (TTS or PTS) in hearing [6]. Of these MAP kinases, JNK and p38 MAPK can function as stress-induced regulators of apoptosis. The protection of inner ear function by JNK inhibitor and p38 MAPK inhibitor after ischemic inner ear damage and NIHL have raised the possibility of using these inhibitors as therapeutic reagents for acute sensorineural hearing loss [7,8,9].

However, comprehensive analyses of MAPK expressions after noise trauma have not been conducted in the *in vivo* cochlea.

Importantly, the precise time course of the regulation of MAP kinases during the development of NIHL is unknown. It is also unknown whether MAP kinases are regulated by transient phosphorylation or *de novo* synthesis of the proteins during this process.

The time course and the mode of regulation of MAP kinase proteins would be critical information to understanding the involvement of MAP kinases in NIHL and the development of therapeutic models for SNHL by interventions into MAP kinase pathways. In the present study, the amount of the phosphorylated proteins – phospho-MEK1, phospho-ERK1/2, phospho-p90 RSK, phospho-JNK, phospho-c-Jun, and phospho-P38 MAPK – as well as that of the total proteins – total-MEK1, total-ERK1/2, total-p90 RSK, total-c-Jun and total-P38 MAPK – were comprehensively analyzed at 0, 3, 6, 12, 24 and 48 h in the mouse cochlea after intense noise exposure. The changes in the hearing threshold showing TTS at 0, 12, and 24 h, and PTS at 14 days were confirmed after the noise trauma. Immunohistochemical data were also sought to delineate in which cochlear structure the active phosphorylated MAP kinases are expressed.

Materials and Methods

Animals

Male CBA/J mice at 10 weeks of age (Jackson Laboratory, Bar Harbor, ME, USA) without any evidence of middle ear infection were used for auditory brainstem response (ABR), protein extraction, and immunohistochemistry examination before and after intense noise exposure. All experimental protocols were approved by Okayama University's Committee on Use and Care of Animals (OKU-2011509) and in accordance with the recommendations of the Weatherall report, "The use of non-human primates in research".

Noise exposure

Animals were exposed, unanesthetized, and unrestrained in a cylindrical sound chamber (33 cm in diameter ×35 cm in height) with a speaker (CF1, Tucker Davis Technologies [TDT], Gainesville, FL, USA) on the top of the chamber. The stimulus of noise exposure was an octave band noise (8.0–16.0 kHz) presented at 120-dB sound pressure level (SPL) for 2 h. The exposure stimulus was generated and filtered with a 60 dB/octave slope by a sound generator (Rp 2.1, TDT), amplified (SA1, TDT), and delivered through the exponential speaker. Sound exposure levels were measured by a sound level meter and confirmed to be 120 dB across any position at the bottom of the cylindrical sound chamber.

ABR threshold determination

One day before (control, $n = 8$) and at 0 h (immediately after the noise exposure, $n = 8$), 12 h ($n = 7$), 24 h ($n = 7$) and 14 days ($n = 6$) after the intense noise exposure, the animals were anesthetized by intraperitoneal injections of ketamine (80 mg/kg) and xylazine (8 mg/kg). ABRs were evoked with clicks through a sound conduction tube and recorded by needle electrodes inserted through the skin (vertex to the ipsilateral retroauricle with a ground at the contralateral retroauricle). The responses were recorded using a signal processor (RA16, TDT). Stimulus sounds were clicks (0.001 ms rise/fall time) with a plateau of 0.1 ms and stimulus rate of 21 Hz. The responses were processed through a 300- to 3,000-Hz bandpass filter and averaged 999 times. The stimuli were applied in 5-dB steps. ABR thresholds were defined as the lowest sound level at which the response peaks clearly presented were read by eye from stacked waveforms.

Quantification of phosphorylated and total MAP kinases using the Bio-Plex® Suspension Array System

The Bio-Plex® Suspension Array System (Bio-Rad Laboratories, Hercules, CA, USA) enables simultaneous quantification of multiple phosphorylated and total proteins in each well of 96-well plates. In this system, an antibody directed against the desired target protein is covalently coupled to internally dyed beads with a fluorescence whose wavelength is specific for each target protein. The beads-coupled antibodies are allowed to react with lysate samples containing the target proteins. Then biotinylated detection antibodies specific for different epitopes of the proteins are added to the reaction, followed by an addition of streptavidin-phycoerythrin (streptavidin-PE). A dual-laser, flow-based microplate reader system (Bio-Plex® 200, Bio-Rad) detects the internal fluorescence of the individual dyed beads and the signal intensity on the bead surface. The relative abundance of the each target protein is reported as the ratio of fluorescence among the wells. In the present study, the abundance of phospho-MEK1, phospho-ERK1/2, phospho-p90 RSK, phospho-JNK, phospho-c-Jun, phospho-P38 MAPK, total-MEK1, total-ERK1/2, total-p90 RSK, total-c-Jun and total-P38 MAPK was simultaneously quantified in the cochlear samples. A specific beads-coupled antibody against mouse total-JNK is not available in the Bio-Plex® Suspension Array System.

Before (control, $n = 8$) and at 0 h ($n = 8$), 3 h ($n = 8$), 6 h ($n = 8$), 12 h ($n = 8$), 24 h ($n = 8$) and 48 h ($n = 8$) after intense noise exposure, the animals were deeply anesthetized by excess ketamine (200 mg/kg). The blood was removed by intracardiac perfusion of PBS and one cochlea per animal was promptly dissected and immediately frozen in liquid nitrogen until protein extraction. The sample tissue was homogenized in the lysis solution of the Bio-Plex® Cell Lysis kit (Bio-Rad) containing PMSF. The sample was sonicated and centrifuged at 4,500 g for 4 min. The supernatant was collected and the protein concentration was determined using the *DC* Protein Assay Kit II (Bio-Rad) and a spectrophotometer. Thirty to fifty mg of total protein was extracted per cochlea. One μL of each diluent containing beads-coupled antibodies against the multiple target proteins was mixed, diluted to a final volume of 50 μL in wash buffer, dispensed into 96-well plates (50 μL per well), and vacuum-filtered. Fifty μL of the protein samples from the cochleae, containing 27.7 μg of the total proteins, was dispensed into the wells, incubated overnight at room temperature, vacuum-filtered, and washed 3 times. Twenty-five μL of the biotinylated detection antibody diluent (25×) was then added, incubated for 30 min, vacuum-filtered and washed 3 times, followed by 50 μL of the streptavidin-PE diluent (100×), incubated for 10 min, and vacuum-filtered. After 3 rinses, 125 μL of the resuspension buffer was added and incubated for 30 min.

The plates were placed on the platform of the Bio-Plex® 200. Using Bio-Plex® Manager software (Bio-Rad), the wavelength of the fluorescence of the coupled beads, which is specific for the each target protein, was detected. The fluorescence from the streptavidin-PE was simultaneously detected and quantified for each target protein. The relative abundance of the target protein was calculated as [fluorescence intensity – background fluorescence] and expressed as the percentage to the mean of the control values from the cochleae that were not exposed to the noise. The data are presented as the means from more than triplicate detection of the proteins.

Immunohistochemistry

After 3 h (for detection of phospho-p90 RSK and phospho-JNK) and 48 h (for detection of phospho-JNK and phospho-p38 MAPK) after the noise exposure, the animals were anesthetized

and perfused intracardially, first with PBS for blood removal, then with 4% paraformaldehyde before the cochleae were dissected. After making small holes at the apex and the round window with a 27-gauge needle, the tissues were immersion-fixed at 4°C for 20 h. They were decalcified in 10% EDTA at 4°C for 4 days, dehydrated through graded alcohol and xylene, and embedded in paraffin. Paraffin sections of 6-μm thickness were dewaxed. Heat-induced epitope retrieval was performed by microwave for 3 min for the detection of phospho-JNK. The sections were incubated with rabbit polyclonal antibody against phospho-p90 RSK(Thr359/Ser363) (×1/250, 9344S, Cell Signaling Technology, Danvers, MA, USA), rabbit polyclonal antibody against phospho-JNK(Thr183/Tyr185) (×1/25, ab4821, Abcam, Cambridge, MA, USA) or rabbit monoclonal antibody against phospho-p38MAPK(Thr180/Tyr182) (×1/50, 4631S, Cell Signaling Technology), 10% normal goat serum, and 1% bovine serum albumin at 4°C overnight. Bound antibody was visualized by the ABC-DAB method (Vectastain Elite ABC kit, Vector Laboratories, Burlingame, CA, USA). Sections after reactions omitting the primary antibody served as the negative controls.

Statistical analysis

For the data analyses of ABR thresholds and the Bio-Plex® Suspension Array System, the data were expressed by dB SPL and the percentages to the mean signal intensities of the control groups(animals without noise exposure), respectively. The differences among all the experimental groups(control, 0, 12, 24 h and 14 days for ABR threshold; control, 0, 3, 6, 12, 24 and 48 h for the Bio-Plex® Suspension Array System) were compared to each other non-parametrically by the Kruskal-Wallis test. Then the differences between the each group and the control group were tested by the Mann-Whitney *U*-test. Statistical significance was assigned to *p*-values of <0.01. Analyses were performed using SPSS software(IBM Corporation, Armonk, NY, USA).

Results

ABR thresholds

ABR thresholds at 0 h (58.1±12.5 dB SPL), 12 h (73.6±14.4), 24 h (48.6±15.7) and 14 days (40.0±13.8) after the intense noise exposure were significantly elevated compared with the control level before the noise exposure (20.6±5.6 dB SPL) at all time points examined (Fig. 1). The temporary threshold shift (TTS) was more severe at 12 h than immediately after the noise exposure, and partial recovery was observed at 24 h. The component of TTS was observed during 0–24 h after the noise exposure. A significant permanent threshold shift (PTS) was confirmed at 14 days after the noise trauma.

Quantification of phosphorylated and total MAP kinases using the Bio-Plex® Suspension Array System

In the present experiments, both phosphorylated and total MAP kinases were quantitatively examined, as phospho- MEK1, ERK1/2, p90 RSK, JNK, c-Jun, and p38 MAPK are the active forms of the each proteins, which further regulate the downstream signaling pathways including several transcription factors.

MEK1

The levels of phospho-MEK1 (Fig. 2A) at 0 h (immediately after the noise exposure; 115.0±7.7; mean±SD; $n=8$; $p<0.01$, compared with the control level), 3 h (214.3±13.3; $p<0.01$), 6 h (200.6±10.8; $p<0.01$), 12 h (161.5±7.3; $p<0.01$), 24 h (145.7±8.4; $p<0.01$), and 48 h (109.2±6.3; $p<0.01$) after the noise exposure (control level; 100.0±4.3) was significantly upregulated to more than 2-fold with a peak surge at 3 h.

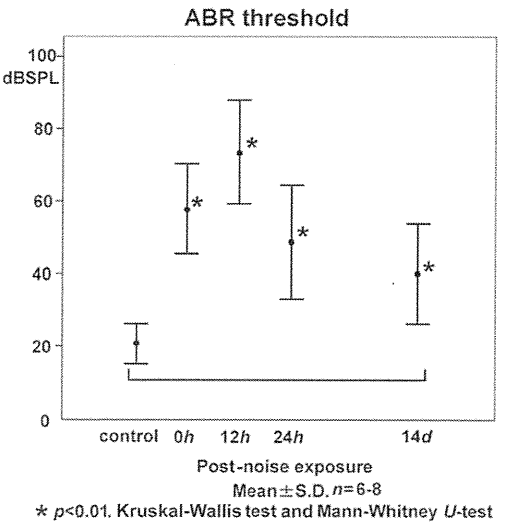

Figure 1. Time course of shifts in the auditory brainstem response (ABR) threshold following exposure to 120-dB octave band noise (8.0–16.0 kHz) for 2 h. Significant elevation of the ABR threshold at 0 h (immediately after the noise exposure; 58.1±12.5 dB sound pressure level (SPL)), 12 h (73.6±14.4), and 24 h (48.6±15.7) exhibited a component of temporary threshold shift (TTS) during 0–24 h. The TTS was more severe at 12 h than at 0 h, and partial recovery was observed at 24 h. A significant permanent threshold shift was confirmed at 14 days (40.0±13.8), compared with the control level before the noise exposure (20.6±5.6 dB SPL).
doi:10.1371/journal.pone.0058775.g001

On the contrary to the surge in the levels of phospho-MEK1, total-MEK1 levels (Fig. 2B) at 0 h (100.9±7.0), 3 h (114.8±3.8), 6 h (109.5±3.8), 12 h (108.4±4.9), 24 h (106.3±3.2), and 48 h (109.3±2.3) after the noise exposure (control level; 100.0±5.5) remained within 100±20% over the time points.

ERK1/2

The levels of phospho-ERK1/2 (Fig. 2C) at 0 h (131.4±11.0; $p<0.01$), 3 h (282.3±16.0; $p<0.01$), 6 h (318.9±18.4; $p<0.01$), 12 h (239.9±13.8; $p<0.01$), 24 h (189.7±14.3; $p<0.01$), and 48 h (103.4±6.6) after the noise exposure (control level; 100.0±4.2) showed more than a 3-fold increase, with a peak at 6 h, whereas total-ERK1/2 levels (Fig. 2D) at 0 h (106.5±7.1), 3 h (117.8±9.1), 6 h (113.8±4.5), 12 h (107.0±5.8), 24 h (101.2±4.9), and 48 h (103.6±7.4) after the noise exposure (control level; 100.0±9.6) were within 100±20% throughout the time points examined.

p90 RSK

The levels of phospho-p90 RSK (Fig. 2E) at 0 h (176.1±14.0; $p<0.01$), 3 h (229.3±18.2; $p<0.01$), 6 h (182.2±8.9; $p<0.01$), 12 h (151.7±11.1; $p<0.01$), 24 h (118.0±8.0; $p<0.01$), and 48 h (115.8±9.2) after the noise exposure (control level; 100.0±9.5) significantly increased to more than 2-fold with a surge at 3 h.

Similarly to the levels of total-MEK1 and total-ERK 1/2, those of total-p90 RSK (Fig. 2F) at 0 h (102.7±6.4), 3 h (104.8±6.5), 6 h (111.5±11.9), 12 h (97.2±7.6), 24 h (89.0±9.6), and 48 h (109.9±8.2) after the noise exposure (control level; 100.0±10.9) remained within 100±20 without any surge throughout the time points.

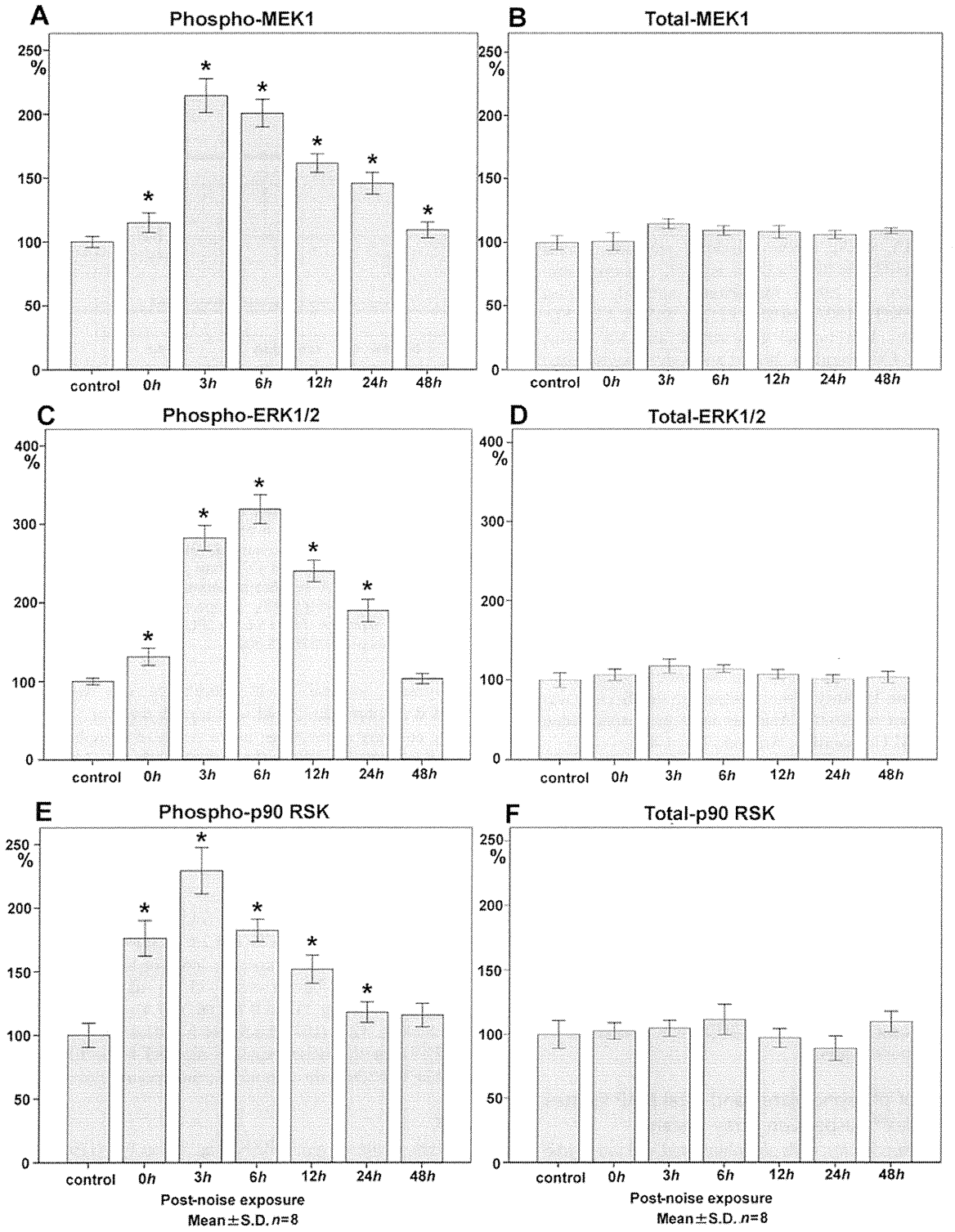

Figure 2. Time course of phospho- and total- MEK1, ERK1/2, p90 RSK expression in the cochlear lysate following exposure to the intense noise. The levels of phospho-MEK1 (**A**) at 0 h (immediately after the noise exposure;115.0±7.7; $p<0.01$), 3 h (214.3±13.3; $p<0.01$), 6 h (200.6±10.8; $p<0.01$), 12 h (161.5±7.3; $p<0.01$), 24 h (145.7±8.4; $p<0.01$), and 48 h (109.2±6.3; $p<0.01$) significantly increased to more than 2-fold after the noise exposure (control level; 100.0±4.3), with a peak surge at 3 h. Total-MEK1 levels (**B**) at 0 h (100.9±7.0), 3 h (114.8±3.8), 6 h (109.5±3.8), 12 h (108.4±4.9), 24 h (106.3±3.2), and 48 h (109.3±2.3) remained within 100±20% of the control level (100.0±5.5) over the time points. The levels of phospho-ERK1/2 (**C**) at 0 h (131.4±11.0; $p<0.01$), 3 h (282.3±16.0; $p<0.01$), 6 h (318.9±18.4; $p<0.01$), 12 h (239.9±13.8; $p<0.01$), 24 h (189.7±14.3; $p<0.01$), and 48 h (103.4±6.6) significantly increased to more than 3-fold after the noise exposure (control level; 100.0±4.3), with a peak surge at 6 h. Total-ERK 1/2 level (**D**) at 0 h (106.5±7.1), 3 h (117.8±9.1), 6 h (113.8±4.5), 12 h (107.0±5.8), 24 h (101.2±4.9), and 48 h (103.6±7.4)

remained within 100±20% of the control level (100.0±9.6) at all time points examined. The levels of phospho-p90 RSK (**E**) at 0 h (176.1±14.0; $p<0.01$), 3 h (229.3±18.2; $p<0.01$), 6 h (182.2±8.9; $p<0.01$), 12 h (151.7±11.1; $p<0.01$), 24 h (118.0±8.0; $p<0.01$), and 48 h (115.8±9.2) significantly increased to more than 2-fold after the noise exposure (control level; 100.0±9.5), with a peak surge at 3 h. Total-p90 RSK levels (**F**) at 0 h (102.7±6.4), 3 h (104.8±6.5), 6 h (111.5±11.9), 12 h (97.2±7.6), 24 h (89.0±9.6) and 48 h (109.9±8.2) remained within 100±20% of the control level (100.0±10.9) without any surge over the time points. (*$p<0.01$, Kruskal-Wallis test and Mann-Whitney *U*-test; $n=8$ for each time point).
doi:10.1371/journal.pone.0058775.g002

JNK

The levels of the phospho-JNK (Fig. 3) in the cochlear lysate at 0 h (104.7±7.6), 3 h (167.2±18.1; $p<0.01$), 6 h (146.4±13.3; $p<0.01$), 12 h (129.2±10.8; $p<0.01$), 24 h (127.1±11.8; $p<0.01$), and 48 h (185.4±13.8; $p<0.01$) after the noise exposure significantly increased from the control level (100.0±11.8), with the early and late peaks at 3 h and 48 h after the noise trauma.

c-Jun

The levels of phospho-c-Jun (Fig. 4A) at 0 h (159.3±11.8; $p<0.01$), 3 h (302.3±14.8; $p<0.01$), 6 h (248.0±18.5; $p<0.01$), 12 h (335.2±31.2; $p<0.01$), 24 h (182.6±14.2; $p<0.01$), and 48 h (106.9±6.1) after the noise exposure (control level; 100.0±7.3) significantly increased with a biphasic surge at 3 h and 12 h.

The levels of total-c-Jun (Fig. 4B) at 0 h (117.3±10.2; $p<0.01$), 3 h (195.7±13.0; $p<0.01$), 6 h (157.0±12.6; $p<0.01$), 12 h (217.4±20.6; $p<0.01$), 24 h (151.2±6.1; $p<0.01$), and 48 h (102.1±7.6) after the noise exposure (control level; 100.0±7.9) showed a significant corresponding biphasic surge to the changes in the levels of phospho-c-Jun.

p38 MAPK

The levels of phospho-p38 MAPK (Fig. 5A) at 0 h (89.2±6.6), 3 h (117.4±13.6), 6 h (103.8±13.6), 12 h (112.6±14.8), 24 h (108.3±11.8), and 48 h (216.3±14.2; $p<0.01$) after the noise exposure (control level; 100.0±13.8) showed a significant late surge at 48 h, to more than 2-fold of the control level.

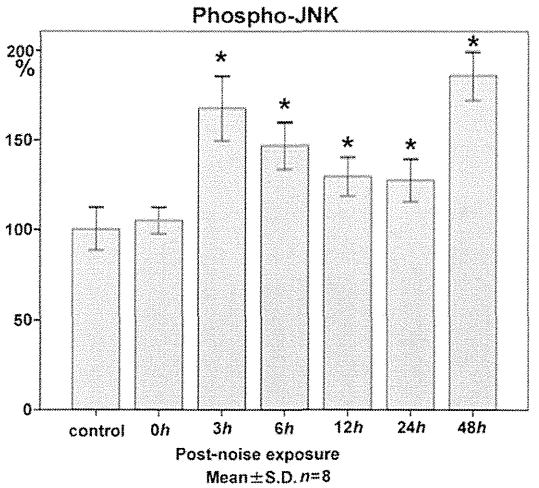

Figure 3. Time course of phospho-JNK expression in the cochlear lysate following exposure to the intense noise. The levels of phospho-JNK in the cochlear lysate at 0 h (immediately after the noise exposure; 104.7±7.6), 3 h (167.2±18.1; $p<0.01$), 6 h (146.4±13.3; $p<0.01$), 12 h (129.2±10.8; $p<0.01$), 24 h (127.1±11.8; $p<0.01$), and 48 h (185.4±13.8; $p<0.01$) after the noise exposure significantly increased from the control level (100.0±11.8), with the early and late peaks at 3 h and 48 h. (*$p<0.01$, Kruskal-Wallis test and Mann-Whitney *U*-test; $n=8$ for each time point).
doi:10.1371/journal.pone.0058775.g003

Total-p38 MAPK levels (Fig. 5B) at 0 h (103.0±10.7), 3 h (134.8±11.6; $p<0.01$), 6 h (124.2±11.7; $p<0.01$), 12 h (116.9±7.1; $p<0.01$), 24 h (111.1±9.9), and 48 h (159.7±12.2; $p<0.01$) after the noise exposure (control level; 100.0±11.9) exhibited a significant surge at 48 h, which corresponds to the late increase in the phospho-p38 MAPK levels. The increase in the level of total-p38 MAPK was also significant at 3 h after the noise trauma.

Immunohistochemistry

As the key markers for each pathway of the MEK1/ERK1/2/p90RSK, JNK/c-Jun, and p38 MAPK cascades, immunolocalizations of phospho-p90RSK, phospho-JNK and phospho-p38 MAPK were investigated in the cochlea. Immunohistochemical examinations were performed at the time points of the peaks in the expression of each phosphorylated protein (at 3 h and 48 h for phospho-JNK, 3 h for phospho-p90 RSK, and 48 h for phospho-p38 MAPK) in the cochlear lysate.

Phospho-JNK

At the early phase of 3 h post-noise exposure, nucleoplasmic and cytoplasmic immunoreactivity to phospho-JNK was observed in the spiral ligament (Fig. 6B), the sensory and supporting cells of the organ of Corti (Fig. 6E; OHC, outer hair cells; IHC, inner hair cells; SC, supporting cells) and the spiral neurons (Fig. 6H). In the spiral ligament, the immunolabeling was more evident in the type I and II fibrocytes (Fig. 6B, arrow) than in the type III and IV fibrocytes (Fig. 6B, arrowhead).

At the late phase of 48 h post-noise trauma, unequivocal immunoreactivity to phospho-JNK was observed in the spiral neurons (Fig. 6K).

Phospho-p90 RSK

At 3 h post-noise trauma, when phospho-p90 RSK expression reached the maximum in the cochlear lysate, immunoreactivity to phospho-p90 RSK was observed in the spiral ligament (Fig. 6C) and in the sensory and supporting cells of the organ of Corti (Fig. 6F). In contrast to phospho-JNK at this time point, no immunolabeling for phospho-p90 RSK was observed in the spiral neuron (Fig. 6I).

Phospho-p38 MAPK

At 48 h post-noise exposure, immunoreactivity to phospho-p38 MAPK was demonstrated in the nucleoplasm and cytoplasm of the spiral neurons (Fig. 6L).

In all experiments to detect the phospho-MAP kinases, no significant signal was observed in the control sections (Fig. 6A, D, G, J).

Discussion

As summarized in Fig. 7, the comprehensive, collated data of MAP kinase expression delineated upregulation of the phospho-MEK1/phospho-ERK1/2/phospho-90 RSK cascade within the early phase of 0–24 h after the noise exposure, which coincided with a TTS. This process did not involve the temporal surge in the levels of total-MEK1, total-ERK1/2 and total-p90 RSK; hence,

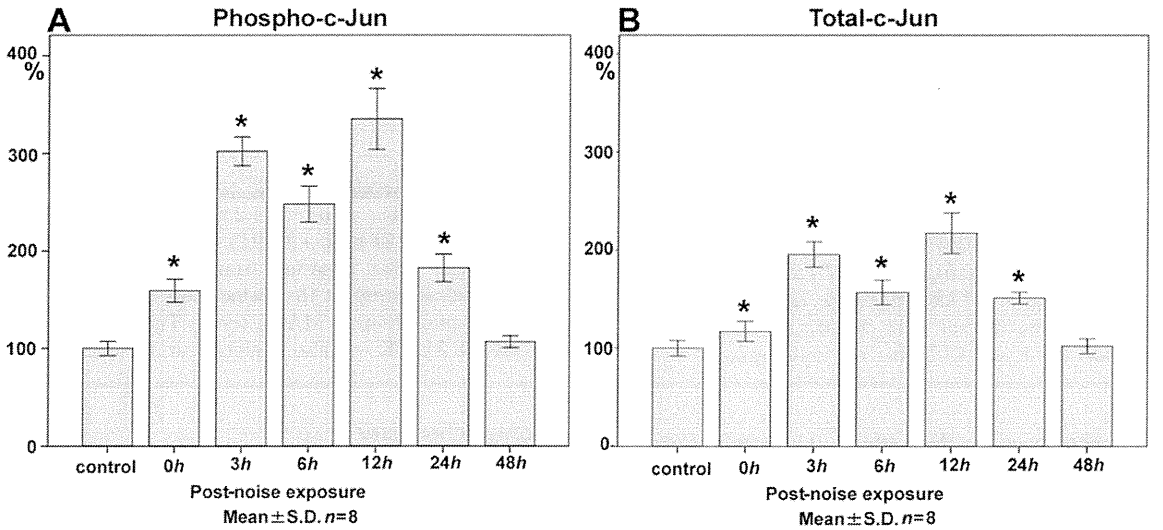

Figure 4. Time course of phospho- and total-c-Jun expression in the cochlear lysate following exposure to the intense noise. The levels of phospho-c-Jun (**A**) in the cochlear lysate at 0 h (immediately after the noise exposure; 159.3±11.8; $p<0.01$), 3 h (302.3±14.8; $p<0.01$), 6 h (248.0±18.5; $p<0.01$), 12 h (335.2±31.2; $p<0.01$), 24 h (182.6±14.2; $p<0.01$), and 48 h (106.9±6.1) after the noise exposure significantly increased from the control level (100.0±7.3) with the biphasic peak at 3 h and 12 h. Total-c-Jun levels (**B**) at 0 h (117.3±10.2; $p<0.01$), 3 h (195.7±13.0; $p<0.01$), 6 h (157.0±12.6; $p<0.01$), 12 h (217.4±20.6; $p<0.01$), 24 h (151.2±6.1; $p<0.01$), and 48 h (102.1±7.6) also showed significant increases from the control level (100.0±7.9) with the biphasic peak, which corresponds to the peaks in phospho-c-Jun at 3 h and 12 h. (*$p<0.01$, Kruskal-Wallis test and Mann-Whitney *U*-test; $n=8$ for each time point).
doi:10.1371/journal.pone.0058775.g004

the upregulation of phospho-MEK1/phospho-ERK1/2/phospho-90 RSK was largely due to transient phosphorylation of the proteins and did not involve *de novo* synthesis of the proteins. Immunohistochemical data showed that the expression of phospho-p90 RSK occurred in the lateral wall (spiral ligament) and in the sensory and supporting cells of the cochlea at 3 h post-noise exposure, at the time of the peak surge of phospho-p90 RSK.

Phospho-JNK and phospho c-Jun, as well as total c-Jun, also showed surges beginning as early as 3 h after the noise exposure. The localization of phospho-JNK was demonstrated in the lateral wall (the spiral ligament), in the sensory and supporting cells of the

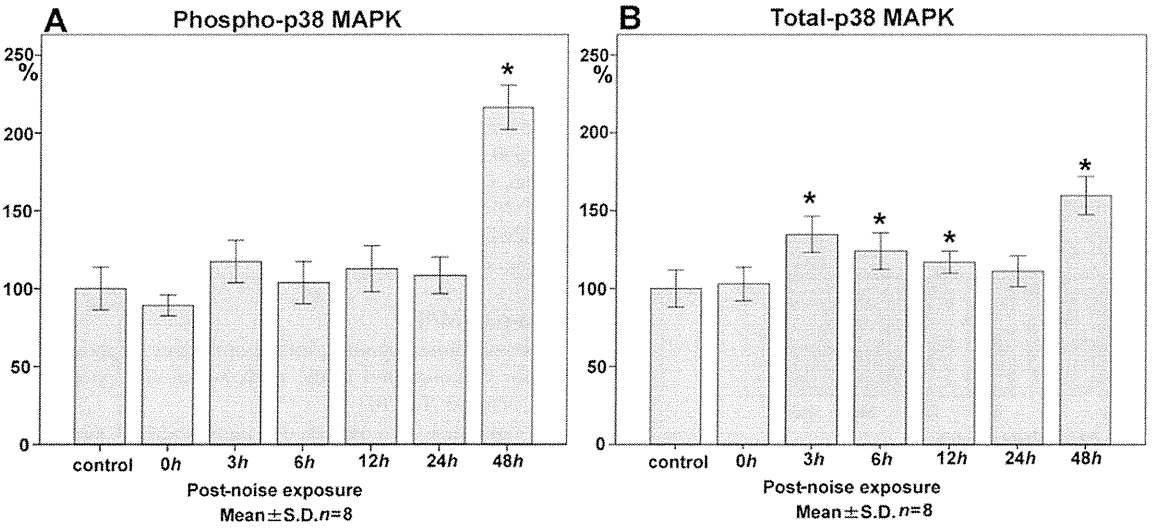

Figure 5. Time course of phospho- and total- p38 MAPK expression in the cochlear lysate following exposure to the intense noise. The levels of phospho-p38 MAPK (**A**) at 0 h (immediately after the noise exposure; 89.2±6.6), 3 h (117.4±13.6), 6 h (103.8±13.6), 12 h (112.6±14.8), 24 h (108.3±11.8), and 48 h (216.3±14.2; $p<0.01$) significantly increased to more than 2-fold of the control level (100.0±13.8) at 48 h after the noise exposure. Total-p38 MAPK levels (**B**) at 0 h (103.0±10.7), 3 h (134.8±11.6; $p<0.01$), 6 h (124.2±11.7; $p<0.01$), 12 h (116.9±7.1; $p<0.01$), 24 h (111.1±9.9), and 48 h (159.7±12.2; $p<0.01$) showed significant increases from the control level (100.0±11.9) at the late phase of 48 h, which coincided with the increase in phospho-p38 MAPK. The upregulation of total-p38 MAPK was also significant at 3 h, followed by 6 h and 12 h after the noise exposure. (*$p<0.01$, Kruskal-Wallis test and Mann-Whitney *U*-test; $n=8$ for each time point).
doi:10.1371/journal.pone.0058775.g005

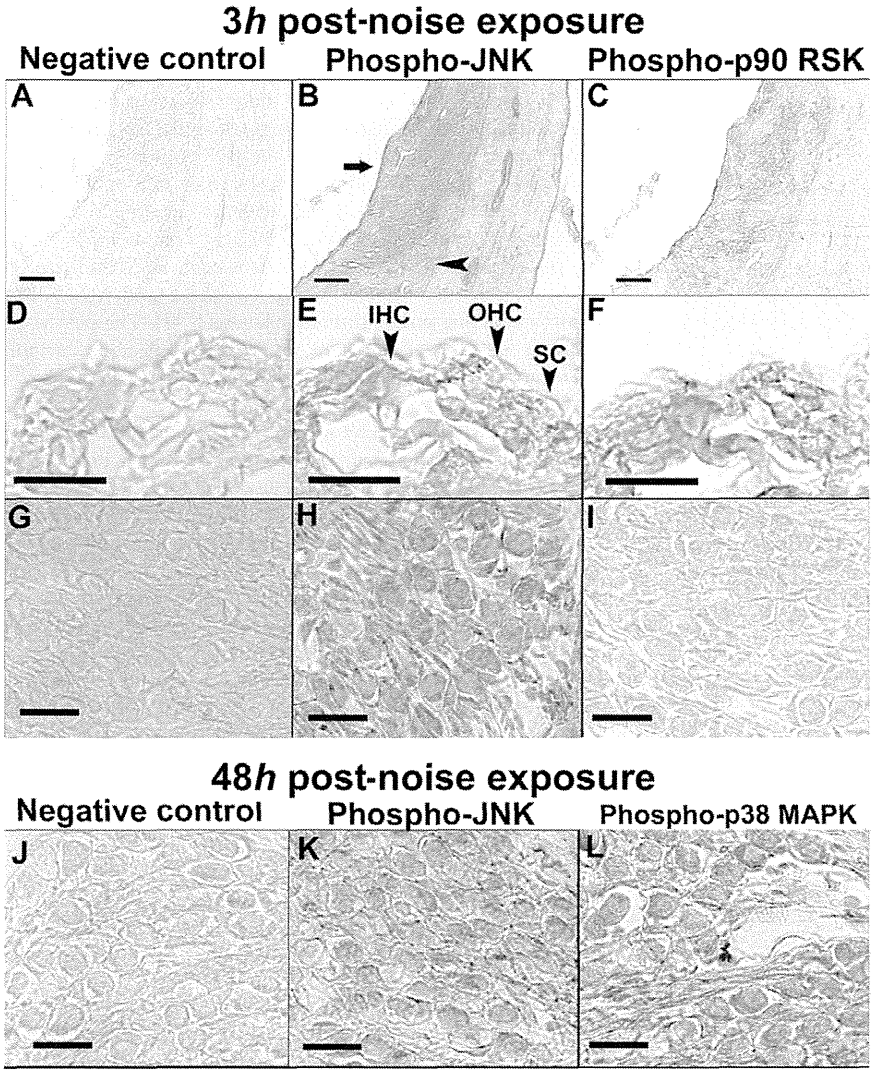

Figure 6. Immunolocalizations of phospho-JNK, phospho-p90 RSK, and phospho-p38 MAPK at 3 h and 48 h after the noise exposure. At 3 h post-noise exposure, cytoplasmic and nucleoplasmic immunoreactivity to phospho-JNK was observed in the spiral ligament (**B**), the sensory and supporting cells of the organ of Corti (**E**; OHC, outer hair cells; IHC, inner hair cells; SC, supporting cells) and the spiral neurons (**H**). In the spiral ligament, phospho-JNK immunoreactivity was more evident in the type I and II fibrocytes (**B, arrow**) than in the type III and IV fibrocytes (**B, arrowhead**). At 3 h post-noise exposure, immunoreactivity to phospho-p90 RSK was demonstrated in the spiral ligament (**C**) and in the sensory and supporting cells of the organ of Corti (**F**). Phospho-p90 RSK immunoreactivity was absent in the spiral neurons at this time point (**I**). At 48 h post-noise exposure, immunolocalization of phospho-JNK was shown in the cytoplasm and nucleoplasm of the spiral neurons (**K**). Phospho-p38 MAPK immunoreactivity in the cytoplasm and nucleoplasm was also demonstrated in the spiral neurons (**L**) at 48 h. The sections of negative controls resulted in no staining in any structures and time points (**A, D, G, J**). Scale bars indicate 20 (**D, E, F, G, H, I, J, K, L**) and 40 (**A, B, C**) μm.
doi:10.1371/journal.pone.0058775.g006

organ of Corti, and in the spiral neurons at 3 h. The upregulation of a downstream effector, phospho-c-Jun, was dependent on the *de novo* synthesis of c-Jun.

In contrast to the upregulation of the phospho-MEK1/phospho-ERK1/2/phospho-90 RSK cascade within 0–24 h, the levels of phospho-JNK and phospho-p38 MAPK also demonstrated significant increases at the late phase of 48 h post-noise exposure. Total-p38 MAPK showed a significant and corresponding increase at 48 h; therefore, the upregulation of phospho-p38 MAPK at 48 h involved *de novo* synthesis of the protein. Immunohistochemical results showed that the expression of phospho-JNK and phospho-p38 MAPK occurred in the spiral neurons of the cochlea at this time point. ABR threshold testing indicated partial recovery of the TTS during the preceding 12–24 h and significant PTS at 14 days post-noise exposure.

Upstream from the MEK1/ERK1/2/p90 RSK signaling pathway, growth factor binding to receptor protein tyrosine kinases in the cell membrane triggers activation of a G-protein, Ras, by exchange of its guanosine diphosphate (GDP) to guanosine triphosphate (GTP) [10]. Activated Ras phosphorylates Raf, and in turn, activated Raf phosphorylates MEK1, leading to the sequential phosphorylation of ERK 1/2 and p90 RSK [11]. p90 RSK is a major downstream effector of the MEK1/ERK1/2 signaling pathway and mediates biological processes such as cell survival, protein synthesis, cell-proliferation, cell growth, and migration through the regulation of transcription factors, c-Fos,

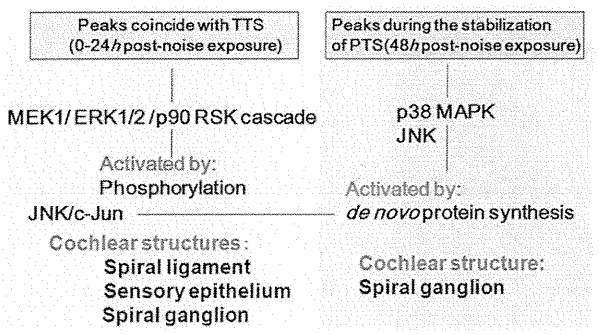

Figure 7. Summary of upregulation of MEK1/ERK1/2/p90 RSK, JNK/c-Jun and p38 MAPK in the cochlea after exposure to the intense noise. The phospho-MEK1/ERK1/2/p90 RSK signaling pathway was activated in the spiral ligament and in the sensory and supporting cells of the organ of Corti, with peaks at 3–6 h and independently of *de novo* synthesis of the protein kinases. The expression of phospho-JNK and p38 MAPK showed late upregulation in the spiral neurons at 48 h, in addition to early upregulation with peaks at 3 h after the noise trauma. Phospho-p38 MAPK and c-Jun activation was dependent on *de novo* synthesis of the proteins.
doi:10.1371/journal.pone.0058775.g007

CREB (cAMP response element binding protein) and NF-kappa B (nuclear factor-kappa B) [12]. p90 RSK activates CREB kinase, which in turn phosphorylates and activates CREB. CREB initiates transcription of survival-promoting genes, including Bcl-2 (B-cell lymphoma 2), Bcl-xL (B-cell lymphoma-extra large) and Mcl1 (myeloid cell leukemia sequence 1), and promotes survival of cultured primary neurons *in vitro* [13,14]. The physiological roles of this signaling pathway suggest that the upregulation of phospho-MEK1/phospho-ERK 1/2/phospho-p90 RSK with the peak surges during 3–6 h, as revealed in the present data, is a protective response to the noise trauma involving the sensory epithelium and the spiral ligament of the cochlea.

Activation of JNK by the upstream kinases MKK4 (MAP kinase kinase 4)/MKK7 [2] can be induced by acoustic trauma [15], ototoxic drugs, and electrode insertion [16] to the inner ear. Phosphorylated JNK binds and phosphorylates downstream effectors such as a transcription factor, c-Jun, ATF2 (activating transcription factor 2), Elk1 (E-twenty six-like transcription factor 1) and p53 (tumor protein 53) [17]. It is reported that these effectors mediate apoptosis in the sensory epithelium and in the lateral wall of the cochlea and neurons [7,15,18]. In the present experiments, phospho-JNK was upregulated in the sensory epithelium, in the lateral wall (the spiral ligament), and in the spiral neurons as early as 3 h post-noise trauma, which is consistent with the previous reports suggesting that the peak expression of phospho-JNK occurred at 0–12 h after the noise exposure that can induce PTS [7,15]. The present data also provides a novel finding of the second, late surge of phospho-JNK in the spiral neurons at 48 h post-noise trauma.

AM111 peptide (which is an equivalent term to D-JNKI-1 peptide) is a cell-permeable compound that inhibits phospho-JNK activity. Intratympanically applied AM111 onto the round window protects hearing from acoustic trauma and prevents ischemic damage to the cochlea [7,8,19]. AM111 is currently under investigation as a potential therapeutic reagent to rescue acute sensorineural hearing loss (http://www.aurismedical.com/, 2013). The present data of the time course of phospho-JNK expression provides significant insight into the design of appropriate therapeutic protocols using the JNK inhibitor.

Phosphorylation of p38 MAPK by the upstream regulators MMK3/MMK6 [2] can be induced by acoustic trauma and aminoglycoside to the cochlea [9,20,21]. Activated p38 MAPK phosphorylates a number of substrates such as MSK1(mitogen- and stress-activated protein kinase 1)/MSK2 and MNK1(MAP kinase interacting serine/threonine kinase 1) [2]. The p38 MAPK signaling pathway shares the downstream effectors, including ATF2 and Elk1, with the JNK pathway and is also involved in apoptosis [17].

The p38 MAPK inhibitors SB202190 and SB203580 dose-dependently decreased hair cell loss and protected hearing after acoustic overexposure of the mouse cochlea [9]. In previous animal studies, the expression of phospho-p38 MAPK was observed in the sensory epithelium at 2–4 h post-noise exposure and the p38 MAPK inhibitors were injected into the mice immediately before the noise exposure [9,21]. These studies have not addressed the cochlear expression of phospho-p38 MAPK for a longer time period than 4 h after noise exposure. The present data for the first time demonstrated the late upregulation of phospho-p38 MAPK in the spiral neurons at 48 h, which is dependent on *de novo* synthesis of the p38 MAPK protein. The phospho-p38MAPK level showed a tendency to increase at 3 h, but was not significant at this time point. We assume that in the present experiments, the sensitivity for detecting phospho-p38 MAPK did not reach the level of significance to show its upregulation in the cochlea at 3 h after noise exposure. The level of total-p38 MAPK demonstrated significant, early upregulation with a peak at 3 h, followed by 6 h and 12 h, which is consistent with previous reports [9,21] and suggestive of the *de novo* protein synthesis.

The present data demonstrated activation of the MEK1/ERK1/2/p90 RSK signaling pathway in the spiral ligament and in the sensory and supporting cells of the organ of Corti, with the peaks occurring at 3–6 h and coinciding with the observed TTS after noise exposure. This process is independent of *de novo* protein synthesis and thought to be a protective response to noise trauma. It is generally accepted that JNK and p38 MAPK act as stress-induced kinases involved in apoptosis. In addition to the early upregulation, with the peak at 3 h after the noise exposure, the present data demonstrated the late upregulations of JNK and p38 MAPK pathways in the spiral neurons at 48 h after the noise trauma. The p38 MAPK activation is dependent on *de novo* protein synthesis. The comprehensive analysis of MAP kinase expression will be critical to understanding the molecular mechanism of NIHL and for developing therapeutic models for acute SNHL.

Author Contributions

Conceived and designed the experiments: YM KF KN. Performed the experiments: YM RO. Analyzed the data: YM KF. Contributed reagents/materials/analysis tools: YM SK. Wrote the paper: YM KF KN.

References

1. Cui Y, Sun GW, Yamashita D, Kanzaki S, Matsunaga T, et al. (2011) Acoustic overstimulation-induced apoptosis in fibrocytes of the cochlear spiral limbus of mice. Eur Arch Otorhinolaryngol 268: 973–978.
2. Cargnello M, Roux PP (2011) Activation and function of the MAPKs and their substrates, the MAPK-activated protein kinases. Microbiol Mol Biol Rev 75: 50–83.
3. Raman M, Chen W, Cobb MH (2007) Differential regulation and properties of MAPKs. Oncogene 26: 3100–3112.

4. Bogoyevitch MA, Ngoei KR, Zhao TT, Yeap YY, Ng DC (2010) c-Jun N-terminal kinase (JNK) signaling: recent advances and challenges. Biochim Biophys Acta 1804: 463–475.
5. Cuadrado A, Nebreda AR (2010) Mechanisms and functions of p38 MAPK signalling. Biochem J 429: 403–417.
6. Meltser I, Tahera Y, Canlon B (2010) Differential activation of mitogen-activated protein kinases and brain-derived neurotrophic factor after temporary or permanent damage to a sensory system. Neuroscience 165: 1439–1446.
7. Wang J, Ruel J, Ladrech S, Bonny C, van de Water TR, et al. (2007) Inhibition of the c-Jun N-terminal kinase-mediated mitochondrial cell death pathway restores auditory function in sound-exposed animals. Mol Pharmacol 71: 654–666.
8. Omotehara Y, Hakuba N, Hato N, Okada M, Gyo K (2011) Protection against ischemic cochlear damage by intratympanic administration of AM-111. Otol Neurotol 32: 1422–1427.
9. Tabuchi K, Oikawa K, Hoshino T, Nishimura B, Hayashi K, et al. (2010) Cochlear protection from acoustic injury by inhibitors of p38 mitogen-activated protein kinase and sequestosome 1 stress protein. Neuroscience 166: 665–670.
10. Zarich N, Oliva JL, Martinez N, Jorge R, Ballester A, et al. (2006) Grb2 is a negative modulator of the intrinsic Ras-GEF activity of hSos1. Mol Biol Cell 17: 3591–3597.
11. Chang F, Steelman LS, Lee JT, Shelton JG, Navolanic PM, et al. (2003) Signal transduction mediated by the Ras/Raf/MEK/ERK pathway from cytokine receptors to transcription factors: potential targeting for therapeutic intervention. Leukemia 17: 1263–1293.
12. Romeo Y, Zhang X, Roux PP (2012) Regulation and function of the RSK family of protein kinases. Biochem J 441: 553–569.
13. Xing J, Ginty DD, Greenberg ME (1996) Coupling of the RAS-MAPK pathway to gene activation by RSK2, a growth factor-regulated CREB kinase. Science 273: 959–963.
14. Bonni A, Brunet A, West AE, Datta SR, Takasu MA, et al. (1999) Cell survival promoted by the Ras-MAPK signaling pathway by transcription-dependent and -independent mechanisms. Science 286: 1358–1362.
15. Nagashima R, Yamaguchi T, Tanaka H, Ogita K (2010) Mechanism underlying the protective effect of tempol and Nω-nitro-L-arginine methyl ester on acoustic injury: possible involvement of c-Jun N-terminal kinase pathway and connexin26 in the cochlear spiral ligament. J Pharmacol Sci 114: 50–62.
16. Eshraghi AA, Wang J, Adil E, He J, Zine A, et al. (2007) Blocking c-Jun-N-terminal kinase signaling can prevent hearing loss induced by both electrode insertion trauma and neomycin ototoxicity. Hear Res 226: 168–177.
17. Mielke K, Herdegen T (2000) JNK and p38 stresskinases – degenerative effectors of signal-transduction-cascades in the nervous system. Prog Neurobiol 61: 45–60.
18. Dragunow M, Young D, Hughes P, MacGibbon G, Lawlor P, et al. (1993) Is c-Jun involved in nerve cell death following status epilepticus and hypoxic-ischaemic brain injury? Brain Res Mol Brain Res 18: 347–352.
19. Coleman JK, Littlesunday C, Jackson R, Meyer T (2007) AM-111 protects against permanent hearing loss from impulse noise trauma. Hear Res 226: 70–78.
20. Wei X, Zhao L, Liu J, Dodel RC, Farlow MR, et al. (2005) Minocycline prevents gentamicin-induced ototoxicity by inhibiting p38 MAP kinase phosphorylation and caspase 3 activation. Neuroscience 131: 513–521.
21. Jamesdaniel S, Hu B, Kermany MH, Jiang H, Ding D, et al. (2011) Noise induced changes in the expression of p38/MAPK signaling proteins in the sensory epithelium of the inner ear. J Proteomics 75: 410–424.

Acta Oto-Laryngologica, 2012; 132: 4–9

informa
healthcare

ORIGINAL ARTICLE

Intratympanic dexamethasone up-regulates *Fkbp5* in the cochleae of mice in vivo

YUKIHIDE MAEDA, KUNIHIRO FUKUSHIMA, SHIN KARIYA, YORIHISA ORITA & KAZUNORI NISHIZAKI

Department of Otolaryngology-Head and Neck Surgery, Okayama University Graduate School of Medicine, Dentistry and Pharmacy, Okayama, Japan

Abstract

Conclusions: Quantitative, real-time RT-PCR demonstrated that intratympanic dexamethasone significantly up-regulates the expression of *Fkbp5* in cochleae of mice in vivo. The immunohistochemistry results showed fundamentally ubiquitous expression of *Fkbp5* in cochlear structures, with relatively strong expression in type 4 fibrocytes and weak signal in the inner hair cells. These data indicate that dexamethasone regulates gene expression at the level of transcription in vivo and that this process is basically ubiquitous in the cochlea. *Objectives:* To demonstrate that intratympanically applied dexamethasone up-regulates *Fkbp5* in the cochlea in vivo. *Methods:* Dexamethasone or control saline were intratympanically applied to adult C57/BL6 mice and dexamethasone-dependent changes in the levels of *Fkbp5* expression in the cochlea were analyzed using quantitative real-time RT-PCR. The expression pattern of *Fkbp5* in cochlea was investigated by immunohistochemistry in mice that were administered dexamethasone and in controls. *Results:* Quantitative real-time RT-PCR demonstrated significant increases of *Fkbp5* expression levels in cochleae of dexamethasone-treated mice as compared with controls at 12 h after application (244.8 ± 155.5, $n = 5$ vs 100.0 ± 3.0, $n = 6$, $p < 0.01$). Immunohistochemistry showed fundamentally ubiquitous expression of *Fkbp5* in cochlear structures, with some strongly positive fibrocytes in the spiral ligaments and weak immunoreactivity in the inner hair cells. Distribution of *Fkbp5* signaling was not different between the dexamethasone-treated group and controls.

Keywords: *Glucocorticoid, gene expression, sensorineural hearing loss, quantitative real-time RT-PCR, immunohistochemistry*

Introduction

Glucocorticoid is a widely used therapeutic drug for acute sensorineural hearing loss (SNHL). A double-blinded placebo study indicated that intratympanically administered dexamethasone may be an effective treatment for idiopathic sudden SNHL [1]. This clinical practice is supported by animal experiments that demonstrated a protective effect of glucocorticoid against inner ear damage caused by ischemia [2], sound trauma [3], and exposure to aminoglycosides [4], cisplatin [5], and salicylate [6].

It is unclear how this protective effect is mediated, although glucocorticoid acts through the glucocorticoid receptor (GR), a member of the nuclear receptor subfamily, to regulate gene expression. GR regulates gene expression via DNA-binding-dependent and -independent pathways. DNA-binding-dependent pathways involve direct binding of GR to the glucocorticoid response element (GRE) in regulatory regions of the genes. DNA-binding-independent pathways control gene expression via the regulation of co-activators and transcription factors [7]. It is also unclear which genes are regulated by glucocorticoid in the cochlea.

FKBP5 is a 51 kDa protein composed of C-terminal tetracopeptide repeat (TPR) domains and peptidyl-prolyl isomerase (PPI) domains [8]. It is a binding

Correspondence: Yukihide Maeda MD PhD, Department of Otolaryngology-Head and Neck Surgery, Okayama University Graduate School of Medicine, Dentistry and Pharmacy, 2-5-1 Shikata-cho, Okayama 700-8558, Japan. Tel: +81 86 235 7307. Fax: +81 86 235 7308. E-mail: maedayj@yahoo.co.jp

(Received 4 July 2011; accepted 21 August 2011)

ISSN 0001-6489 print/ISSN 1651-2251 online
DOI: 10.3109/00016489.2011.619571

partner of FK506, a potent immunosuppressant. Through the function of the TPR and PPI domains, FKBP5 is involved in processes such as the regulation of steroid hormone receptor function [9], the regulation of microtubule dynamics [10], the inhibition of apoptosis [11], and the interaction with channels of the transient receptor potential canonical (TRPC) subfamily [8].

In the present study we examined dexamethasone regulation of *Fkbp5* expression in the cochlea in vivo for the following reasons. First, we demonstrated in an earlier work that *Fkbp5* is one of the most remarkably up-regulated genes by dexamethasone in cultured cochlear tissue in vitro. *Fkbp5* expression was up-regulated to approximately sixfold of the control level in the presence of dexamethasone in mouse cochlear explants, as identified by DNA microarray screening [12]. Second, *Fkbp5* is a suitable biomarker, which demonstrates that dexamethasone regulates gene expression at the level of transcription via DNA-binding-dependent pathways. The *Fkbp5* gene possesses 12 GREs in its up- and downstream regulatory regions. Binding of GR to these GREs enhances transcription of *Fkbp5* in vitro in cultured cells. FKBP5 is up-regulated within 3 h after the application of dexamethasone and this effect continues up to 24 h in A549 cells [13]. Third, the FKBP5 protein is suggested to be involved in the hearing processes of the cochlea. FKBP5 forms a tight complex with FK506 and inhibits it [14]. FK506 can cause SNHL in liver transplant recipients [15]. It is thought that FKBP5 also possesses physiological roles relevant to sound transduction processes in the cochlea.

To elucidate the mechanism of action of glucocorticoid in the cochlea, it is critical to understand how glucocorticoid regulates gene expression in the cochlea. In the present study, we showed that the transcription of *Fkbp5* was robustly up-regulated by intratympanic application of dexamethasone into the cochlea in vivo, using quantitative real-time RT-PCR. Immunohistochemical data for *Fkbp5* expression was also shown to provide a clue to understanding glucocorticoid action in the cochlea.

Material and methods

Intratympanic application of dexamethasone

Female C57/BL6 mice (P45-50) were anesthetized with intraperitoneal injections of ketamine (75 mg/kg) and medetomidine hydrochloride (15 mg/kg). The surgical approach to the round window membrane (RWM) was performed according to Jero et al. with minor modifications [16]. A paramedial sagittal incision was performed in the right ventral neck. The submandibular gland was laterally displaced. The facial vein and nerve were visualized laterally to the digastric muscle, as well as the common carotid artery, the internal jugular vein, and the hypoglossal nerve between the digastric muscle and the trachea [16]. The caudal-lateral portion of the posterior belly of the digastric muscle was cut by electric cautery (MediChoice, Arron Medical, St Petersburg, FL, USA) to expose the tympanic bulla. A small hole was made in the bulla using electric cautery and a 23-gauge needle. The RWM and round window niche were then directly visualized caudally to the stapedial artery.

Dexamethasone sodium phosphate in saline (24 mg/ml, 5 µl, $n = 5$) or control saline (5 µl, $n = 6$) were injected into the tympanic cavity around the RWM using a microsyringe (Hamilton, Reno, NV, USA). A small piece of gelfoam was placed in the tympanic cavity and the hole in the tympanic bulla was sealed with gelfilm. At 12 h after the application, the cochleae were promptly dissected and frozen in liquid nitrogen until time of RNA extraction. Remaining animals were processed for immunohistochemistry. All experimental protocols were in compliance with the guidelines of Okayama University's Committee on Use and Care of Animals.

Quantitative real-time RT-PCR

Total RNA was purified from cochlear tissue using RNeasy columns (Qiagen, Hilden, Germany) and treated with DNaseI. Usually 300–400 ng total RNA was extracted per cochlea. Reverse transcription was performed with 20 ng of total RNA samples using random primers and MultiScribe™ reverse transcriptase from the High Capacity cDNA Archive kit (Applied Biosystems, Foster City, CA, USA), as described by the manufacturer. Specific PCR primers and the TaqMan probe for *Fkbp5* were selected from a pre-designed TaqMan Gene Expression Assay system (TaqMan Gene Expression Assay ID: Mm01300964 m1, Applied Biosystems). The PCR reaction mix included gene-specific primers (900 nM), 6-FAM™ dye-labeled TaqMan probe (250 nM), and TaqMan Universal PCR Master Mix containing AmpliTaq Gold DNA polymerase. Hot-start two-step PCR consisting of preheating at 95°C for 10 min, denaturing at 95°C for 15 s, and annealing and extension at 60°C for 1 min was performed using a 7500 Fast Real-time PCR systems (Applied Biosystems).

Relative abundance of specific mRNAs in the cochlear samples was calculated from the difference in Ct value (cycling threshold, the thermocycling

number at which the fluorescence of 6-FAM™ released from the TaqMan probe became a determined level). The Ct value in each sample was determined as the mean of the data from triplicate experiments. Data were normalized to the expression levels of the internal control, mouse 18S rRNA. The difference between the groups was examined by Student's *t* test. Statistical significance was assigned to *p* values of <0.01.

Immunohistochemistry

At 12 h after intratympanic application of dexamethasone (n = 3) or saline (n = 3), the animals were anesthetized and perfused intracardially first with phosphate-buffered saline (PBS) for blood removal, then with 4% paraformaldehyde before cochleae were dissected. After making small holes at the apex and the round window with a 27-gauge needle, the tissues were immersion-fixed at 4°C for 16 h. They were decalcified in 0.2 M EDTA at 4°C for 48 h, dehydrated through graded alcohol and xylene, and embedded in paraffin. Paraffin sections of 6 μm thickness were dewaxed and heat-induced epitope retrieval was performed by microwave for 3 min. The sections were incubated with a rabbit polyclonal antibody against *Fkbp5* (5 μg/ml, ab46002, Abcam, Cambridge, MA, USA) or control non-specific rabbit IgG (5 μg/ml), 10% normal goat serum, and 1% bovine serum albumin at 4°C overnight. Bound antibody was visualized by the ABC-DAB method (Vectastain Elite ABC kit, Vector Laboratories, Burlingame, CA, USA).

Results

Quantitative real-time RT-PCR

The detection of gene expressions by real-time RT-PCR resulted in stable amplification curves, validating specific and sensitive detection of *Fkbp5* and the internal control of mRNAs. In Figure 1A, blue represents the amplification curves of *Fkbp5*, red represents those of mouse 18S rRNA, and the green line indicates the signal intensity at which the Ct values were determined.

The quantitative analysis of the real-time RT-PCR data revealed an approximately 2.4-fold increase of *Fkbp5* expression levels in the cochleae of the dexamethasone-treated group, as compared with those of the saline-treated control group (244.8 ± 155.5, n = 5 vs 100.0 ± 3.0, n = 6). The difference in *Fkbp5* expression between the two groups was highly significant (p < 0.01) (Figure 1B).

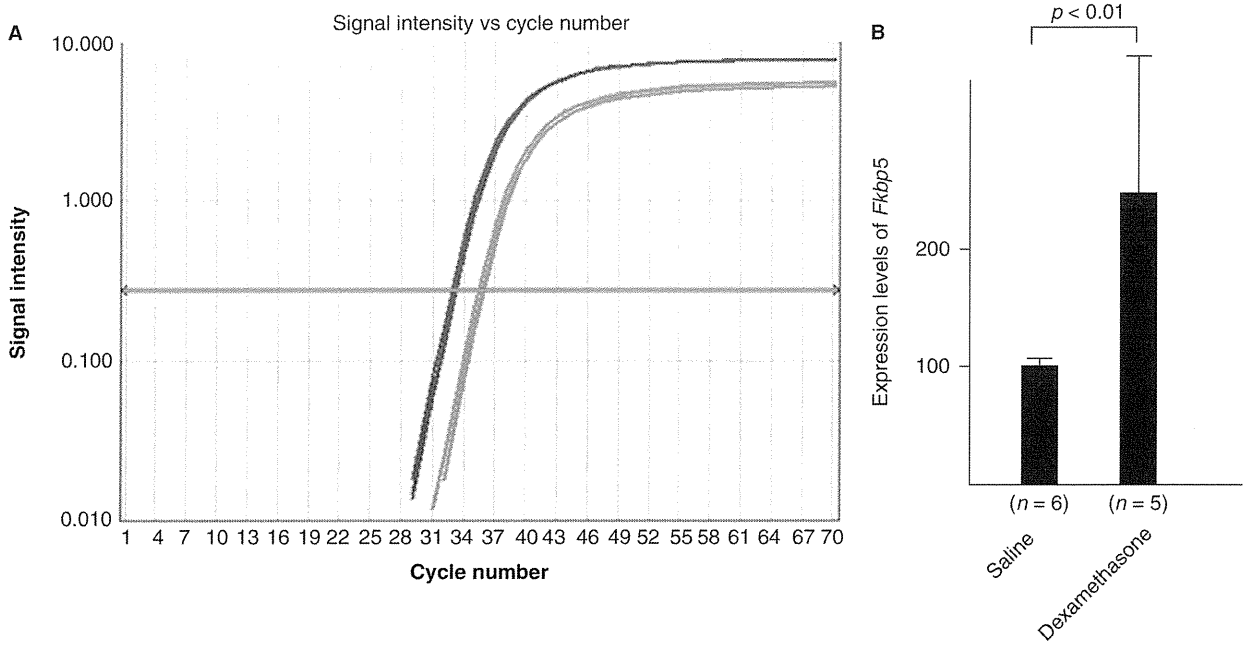

Figure 1. Detection and quantification of *Fkbp5* mRNA and 18S rRNA by real-time RT-PCR. The real-time RT-PCR resulted in consistent amplification curves of *Fkbp5* (blue) mRNA and the internal control, mouse 18S rRNA (red), confirming specific and reliable detection of target RNAs. The green line indicates the signal level at which Ct values for quantitative analysis was determined (A). Quantitative analysis of the real-time RT-PCR results revealed that *Fkbp5* expression was up-regulated by approximately 2.4-fold in the cochleae of the dexamethasone-treated mice in vivo as compared with those of the control mice at 12 h after the application (244.8 ± 155.5, n = 5 vs 100.0 ± 3.0, n = 6, p < 0.01, Student's t test) (B).

Immunohistochemistry

Figure 2 represents the immunohistochemical results in the dexamethasone-treated animals. As shown in low-power view in Figure 2A, specific *Fkbp5*-like immunoreactivities throughout the cochlear structures were detected by immunohistochemistry. Figure 2B shows completely negative staining in the controls incubated with non-specific rabbit IgG, confirming the visible staining to be highly specific for *Fkbp5*.

The high-power views in Figure 2C–H illustrate predominantly cytoplasmic *Fkbp5*-like immunoreactivities

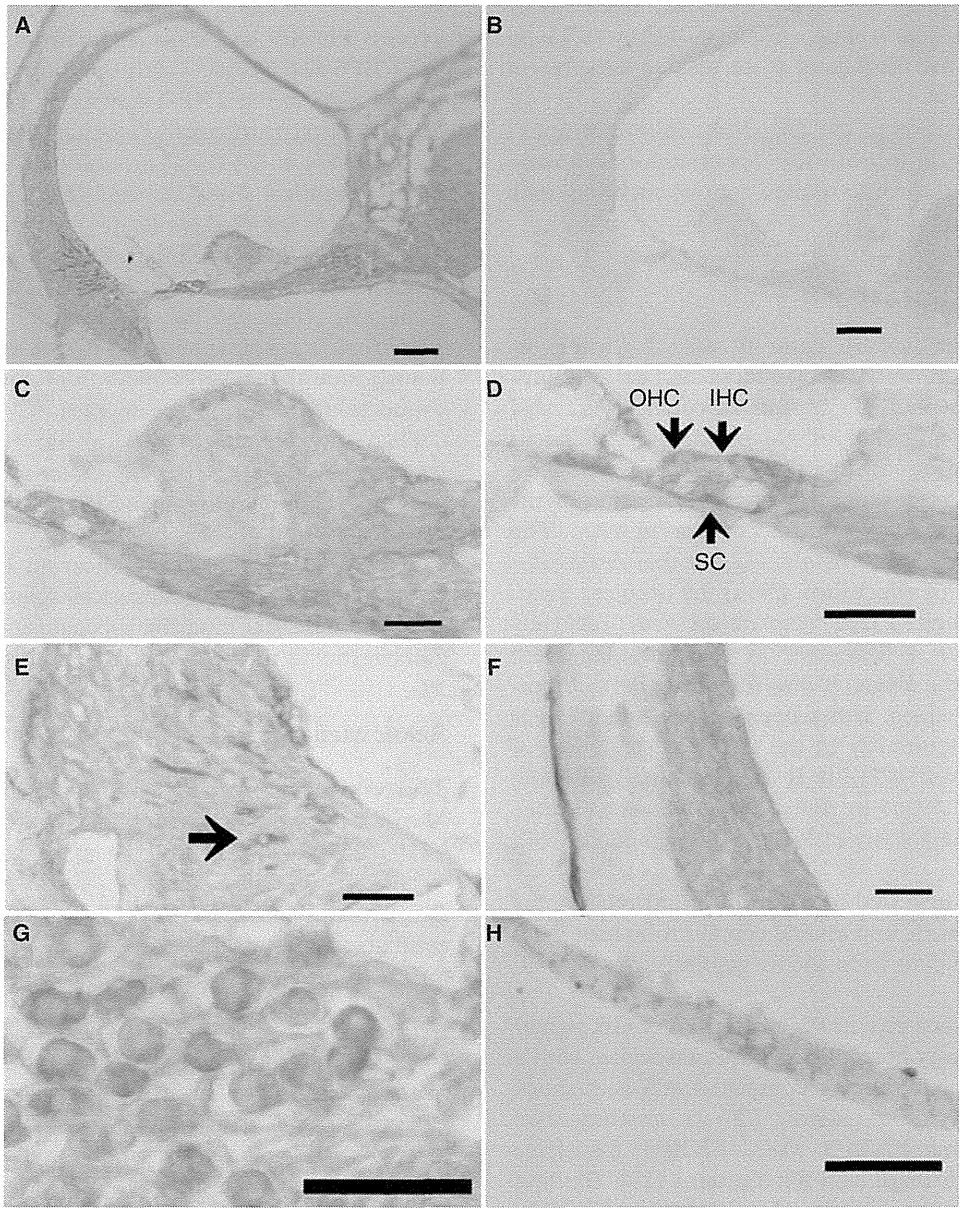

Figure 2. Low- and high-power views of *Fkbp5*-like immunoreactivity in the cochlea. Low-power view in (A) illustrates specific signaling for *Fkbp5* throughout the cochlear structures of the dexamethasone-treated mice. (B) The absence of immunostaining in the negative controls incubated with non-specific rabbit IgG, confirming that the visualized immunostaining was highly specific for *Fkbp5*. Scale bars in A and B, 0.1 mm. (C–H) High-power views show predominantly cytoplasmic signaling specific for *Fkbp5* in the spiral limbus (C), organ of Corti (D), spiral ligament (E), stria vascularis (F), spiral neurons (G), and Reissner's membrane (H). In the organ of Corti (D), unequivocal immunoreactivity was observed in the outer hair cells (OHC) and supporting cells (SC), whereas specific signaling was weak in the inner hair cells (IHC). In the spiral ligament (E), some type 4 fibrocytes showed intense immunoreactivity (arrow). Scale bars in C–H, 40 μm. The distribution of the *Fkbp5*-like immunoreactivity was the same in the dexamethasone-treated animals and the saline-treated controls (data not illustrated).

in the spiral limbus (C), organ of Corti (D), spiral ligament (E), stria vascularis (F), spiral neurons (G), and Reissner's membrane (H). In the organ of Corti (Figure 2D), specific signaling for *Fkbp5* was unequivocal in the outer hair cells (OHCs) and the supporting cells (SCs), whereas the immunoreactivity was weak in the inner hair cells (IHCs). In the spiral ligament (Figure 2E), some type 4 fibrocytes exhibited strong immunoreactivity in the cytoplasm (arrow). These strongly positive fibrocytes were also remarkable at low-power view.

The distribution of the *Fkbp5*-like immunoreactivity was identical in both the dexamethasone-treated cochleae and the saline-treated control cochleae (data not illustrated).

Discussion

The present data clearly demonstrated that intratympanic administration of dexamethasone robustly upregulates expression of *Fkbp5* in the cochlea. As *Fkbp5* serves as a biomarker of glucocorticoid-dependent induction of transcription, these data strongly suggest that dexamethasone controls gene expression at the level of transcription in the cochlea in vivo. The immunohistochemical results suggest that dexamethasone exerts this effect throughout the cochlear structures. Although *Fkbp5* expression was relatively strong in type 4 fibrocytes in the spiral ligament and weak in the IHCs, it was fundamentally ubiquitous in the cochlea. It has been reported that GR is expressed ubiquitously in the cochlear structures of murines as well [17]. It is also assumed that the expression of *Fkbp5* in the cochleae of control mice may reflect the activity of endogenous glucocorticoid in vivo.

FKBP5 is suggested to have important roles in the process of hearing, and several cellular roles have been implicated, mainly from the viewpoint of its domain structure.

FKBP5 plays a role in the regulation of GR signaling. Cytoplasmic hormone-free GR associates with a super-chaperone complex composed of a heat-shock protein 90 (HSP90) dimer, P23 (a co-chaperone molecule), and FKBP5 [18]. FKBP5 associates with HSP90 through its TRP domains [19]. Binding of glucocorticoid to GR transfers FKBP5 to FKBP52 in the super-chaperone complex and converts GR to its DNA-binding form [9]. Therefore glucocorticoid-induced FKBP5 forms a short feedback loop to maintain hormone-free GR.

FKBP5 regulates microtubule dynamics through its PPI activity on tau configuration. Isomerization of tau enhances tau dephosphorylation, and dephosphorylated tau is recycled to microtubules and stabilizes them. Therefore FKBP5 promotes stabilization of microtubules [10].

FKBP5 is also involved in apoptosis resistance in in vitro cultured cells. In cultured melanoma cells depleted of FKBP5 by RNA interference, active caspase 3 and 7 were up-regulated and radiation-induced apoptosis was activated. This process is suppressed in cells, such as melanoma cells, that express FKBP5 and show high chronogenicity [11].

FKBP5 also interacts with and influences ion channel proteins of the TRPC subfamily. FKBP5 inhibits calcium entry through the Isoc channel, of which at least TRPC1 and TRPC4 are subunits [8]. An immunohistochemical study showed that Trpc1 and 4 are expressed in the cochlea [20].

Through these cellular functions, FKBP5 is thought to contribute to the physiological process of hearing. Since SNHL is a reported side effect of FK506 in patients [15] and FKBP5 inhibits FK506, it is suggested that FKBP5 plays important roles in the sound transduction in the cochlea.

Data showing that intratympanic dexamethasone robustly induces *Fkbp5* expression indicated that dexamethasone controls gene expression at the level of transcription in the cochlea in vivo. FKBP5 is suggested to be relevant to hearing functions and investigation of its physiological roles will provide clues to understanding the mechanisms of action of glucocorticoid in the cochlea.

Acknowledgments

This work was supported by a grant from Japanese Ministry of Health, Labour and Welfare (H23-NANCHI-IPPAN-021).

Declaration of interest: The authors report no conflicts of interest. The authors alone are responsible for the content and writing of the paper.

References

[1] Plontke SK, Lowenheim H, Mertens J, Engel C, Meisner C, Weidner A, et al. Randomized, double blind, placebo controlled trial on the safety and efficacy of continuous intratympanic dexamethasone delivered via a round window catheter for severe to profound sudden idiopathic sensorineural hearing loss after failure of systemic therapy. Laryngoscope 2009;119:359–69.

[2] Morawski K, Telischi FF, Bohorquez J, Niemczyk K. Preventing hearing damage using topical dexamethasone during reversible cochlear ischemia: an animal model. Otol Neurotol 2009;30:851–57.

[3] Takemura K, Komeda M, Yagi M, Himeno C, Izumikawa M, Doi T, et al. Direct inner ear infusion of dexamethasone attenuates noise-induced trauma in guinea pig. Hear Res 2004;196:58–68.

[4] Himeno C, Komeda M, Izumikawa M, Takemura K, Yagi M, Weiping Y, et al. Intra-cochlear administration of dexamethasone attenuates aminoglycoside ototoxicity in the guinea pig. Hear Res 2002;167:61–70.
[5] Daldal A, Odabasi O, Serbetcioglu B. The protective effect of intratympanic dexamethasone on cisplatin-induced ototoxicity in guinea pigs. Otolaryngol Head Neck Surg 2007;137:747–52.
[6] Park SK, Choi D, Russell P, John EO, Jung TT. Protective effect of corticosteroid against the cytotoxicity of aminoglycoside otic drops on isolated cochlear outer hair cells. Laryngoscope 2004;114:768–71.
[7] Muzikar KA, Nickols NG, Dervan PB. Repression of DNA-binding dependent glucocorticoid receptor-mediated gene expression. Proc Natl Acad Sci U S A 2009;106:16598–603.
[8] Cioffi DL, Hubler TR, Scammell JG. Organization and function of the FKBP52 and FKBP51 genes. Curr Opin Pharmacol 2011;11:1–6.
[9] Davies TH, Ning YM, Sanchez ER. A new first step in activation of steroid receptors: hormone-induced switching of FKBP51 and FKBP52 immunophilins. J Biol Chem 2002;277:4597–600.
[10] Jinwal UK, Koren J 3rd, Borysov SI, Schmid AB, Abisambra JF, Blair LJ, et al. The Hsp90 cochaperone, FKBP51, increases Tau stability and polymerizes microtubules. J Neurosci 2010;30:591–9.
[11] Romano S, D'Angelillo A, Pacelli R, Staibano S, De Luna E, Bisogni R, et al. Role of FK506-binding protein 51 in the control of apoptosis of irradiated melanoma cells. Cell Death Differ 2010;17:145–57.
[12] Maeda Y, Fukushima K, Hirai M, Kariya S, Smith RJ, Nishizaki K. Microarray analysis of the effect of dexamethasone on murine cochlear explants. Acta Otolaryngol 2010;130:1329–34.
[13] Paakinaho V, Makkonen H, Jaaskelainen T, Palvimo JJ. Glucocorticoid receptor activates poised FKBP51 locus through long-distance interactions. Mol Endocrinol 2010;24:511–25.
[14] Weiwad M, Edlich F, Kilka S, Erdmann F, Jarczowski F, Dorn M, et al. Comparative analysis of calcineurin inhibition by complexes of immunosuppressive drugs with human FK506 binding proteins. Biochemistry 2006;45:15776–84.
[15] Rifai K, Kirchner GI, Bahr MJ, Cantz T, Rosenau J, Nashan B, et al. A new side effect of immunosuppression: high incidence of hearing impairment after liver transplantation. Liver Transpl 2006;12:411–15.
[16] Jero J, Tseng CJ, Mhatre AN, Lalwani AK. A surgical approach appropriate for targeted cochlear gene therapy in the mouse. Hear Res 2001;151:106–14.
[17] Shimazaki T, Ichimiya I, Suzuki M, Mogi G. Localization of glucocorticoid receptors in the murine inner ear. Ann Otol Rhinol Laryngol 2002;111:1133–8.
[18] Silverstein AM, Galigniana MD, Chen MS, Owens-Grillo JK, Chinkers M, Pratt WB. Protein phosphatase 5 is a major component of glucocorticoid receptor.hsp90 complexes with properties of an FK506-binding immunophilin. J Biol Chem 1997;272:16224–30.
[19] Denny WB, Prapapanich V, Smith DF, Scammell JG. Structure-function analysis of squirrel monkey FK506-binding protein 51, a potent inhibitor of glucocorticoid receptor activity. Endocrinology 2005;146:3194–201.
[20] Takumida M, Anniko M. Expression of canonical transient receptor potential channel (TRPC) 1-7 in the mouse inner ear. Acta Otolaryngol 2009;129:1351–8.

Notice of correction

Figure 2 panel D has been amended from the Early Online version of this paper published 25 October 2011.

PLOS ONE

Novel *In Vivo* Imaging Analysis of an Inner Ear Drug Delivery System in Mice: Comparison of Inner Ear Drug Concentrations over Time after Transtympanic and Systemic Injections

Sho Kanzaki[1*☯], Masato Fujioka[1☯], Akimasa Yasuda[2], Shinsuke Shibata[3], Masaya Nakamura[2], Hirotaka James Okano[3], Kaoru Ogawa[1], Hideyuki Okano[3]

1 Department of Otolaryngology Head and Neck Surgery, Keio University, Shinjuku-ku, Tokyo, Japan, **2** Department of Orthopedics, School of Medicine, Keio University, Shinjuku-ku, Tokyo, Japan, **3** Department of Physiology, School of Medicine, Keio University, Shinjuku-ku, Tokyo, Japan

Abstract

Objective: Systemic steroid injections are used to treat idiopathic sudden-onset sensorineural hearing loss (ISSHL) and some inner ear disorders. Recent studies show that transtympanic (TT) steroid injections are effective for treating ISSHL. As *in vivo* monitoring of drug delivery dynamics for inner ear is lacking, its time course and dispersion of drugs is unknown. Here, we used a new *in vivo* imaging system to monitor drug delivery in live mice and to compare drug concentrations over time after TT and systemic injections.

Methods: Luciferin delivered into the inner ears of GFAP-Luc transgenic mice reacted with luciferase in GFAP-expressing cells in the cochlear spiral ganglion, resulting in photon bioluminescence. We used the Xenogen IVIS® imaging system to measure how long photons continued to be emitted in the inner ear after TT or systemic injections of luciferin, and then compared the associated drug dynamics.

Results: The response to TT and IP injections differed significantly. Photons were detected five minutes after TT injection, peaking at ~20 minutes. By contrast, photons were first detected 30 minutes after i.p. injection. TT and i.p. drug delivery time differed considerably. With TT injections, photons were detected earlier than with IP injections. Photon bioluminescence also disappeared sooner. Delivery time varied with TT injections.

Conclusions: We speculate that the drug might enter the Eustachian tube from the middle ear. We conclude that inner-ear drug concentration can be maintained longer if the two injection routes are combined. As the size of luciferin differs from that of therapeutics like dexamethasone, combining drugs with luciferin may advance our understanding of *in vivo* drug delivery dynamics in the inner ear.

Citation: Kanzaki S, Fujioka M, Yasuda A, Shibata S, Nakamura M, et al. (2012) Novel *In Vivo* Imaging Analysis of an Inner Ear Drug Delivery System in Mice: Comparison of Inner Ear Drug Concentrations over Time after Transtympanic and Systemic Injections. PLoS ONE 7(12): e48480. doi:10.1371/journal.pone.0048480

Editor: Demetrios Vavvas, Massachusetts Eye & Ear Infirmary, Harvard Medical School, United States of America

Received August 3, 2012; **Accepted** October 2, 2012; **Published** December 12, 2012

Funding: This work was supported by a grant from the Ministry of Health, Labor and Welfare (KO 2011) and by a grant from the Ministry of Education, Culture, Sports, Science and Technology (KO 2012). The funders had no role in study design, data collection and analysis, decision to publish, or preparation of the manuscript.

Competing Interests: The authors have declared that no competing interests exist.

* E-mail: skan@a7.keio.jp

☯ These authors contributed equally to this work.

Introduction

Sensorineural hearing loss is mostly caused by inner ear disorders. Systemic injection of steroids is generally used in inner ear diseases, especially idiopathic sensorineural hearing loss. Recent studies show that an approach for drug delivery through the tympanic membrane to the round window (RW) into the inner ear is as effective as systemic injections [1]. However, there are a few studies examining the pharmacokinetics of inner ear drug delivery, and the time course remains elusive. Patients with hearing loss also exhibit a significant rate of RW obstruction, suggesting that drugs may not infiltrate the cochlea in these cases [2] [3]. When the RW is covered with connective tissue, we expect drug delivery into the inner ear can be facilitated.

Several animal experiment studies have been performed, but the inner ear has a very small volume of fluid, even when including both perilymph and endolymph (total 0.19 μl in mouse [4]). This makes reliable measurement difficult.

Microdialysis is an effective way for analyzing the cochlear fluid of animals. It has the advantage of making repeated measurements possible, allowing drug time course determination, preventing measurement artifacts arising through perilymph volume loss due to leaks, and lessens disturbance of perilymph due to the low volumes of drug recovery. However, there are several limitations